NATIONAL ADVISORY COMMITTEE FOR AERONAUTICS

TECHNICAL NOTE 2425

PLASTIC STRESS-STRAIN RELATIONS FOR 75S-T6 ALUMINUM ALLOY SUBJECTED TO BIAXIAL TENSILE STRESSES

By Joseph Marin, B. H. Ulrich, and W. P. Hughes

The Pennsylvania State College

Washington

August 1951

NATIONAL ADVISORY COMMITTEE FOR AERONAUTICS

TECHNICAL NOTE 2425

PLASTIC STRESS-STRAIN RELATIONS FOR 75S-T6 ALUMINUM ALLOY SUBJECTED TO BIAXIAL TENSILE STRESSES

By Joseph Marin, B. H. Ulrich, and W. P. Hughes

SUMMARY

In this investigation, the material tested was a 75S-T6 aluminum alloy and the stresses were essentially biaxial and tensile. The biaxial tensile stresses were produced in a specially designed testing machine by subjecting a thin-walled tubular specimen to axial tension and internal pressure. Plastic stress-strain relations for various biaxial stress conditions were obtained using a clip-type SR-4 strain gage.

Three types of tests were made: Constant-stress-ratio tests, variable-stress-ratio tests, and special tests. The constant-stress-ratio test results gave control data and showed the influence of biaxial stresses on the yield, fracture, and ultimate strength of the material. By means of the variable-stress-ratio tests, it is possible to determine whether there is any significant difference between the flow and deformation type of theory. Finally, special tests were conducted to check specific assumptions made in the theories of plastic flow.

The constant-stress-ratio tests show that the deformation theory based on the octahedral, effective, or significant stress-strain relations is in approximate agreement with the test results. The variable-stress-ratio tests show that both the deformation and flow theory are in equally good agreement with the test results.

INTRODUCTION

Machine and structural parts may be subjected to stresses beyond the yield strength of the material. Often these stresses are not simple stresses acting in one direction, but are combined stresses acting in more than one direction. To adequately determine the factors of safety in a particular member, it is necessary to know the plastic stress-strain relations. Furthermore, in parts which are subjected to initial residual

stresses, such as high-pressure vessels, information on the plastic stress-strain relations is important. Another valuable use of the plastic stress-strain relation in metals is in the study and improvement of forming operations.

In recent years, many theories have been proposed for defining the plastic combined stress-strain relations for metals based on the simple-tension stress-strain relations. These theories are needed for the solution of the engineering problems mentioned in the foregoing paragraph. However, for engineering design purposes, it is desirable to know which of the available theories, if any, agree with the test results for the various possible stress conditions. In the past, most investigations have been made for biaxial tension stresses and for the condition in which the ratio of the principal stresses remains constant during loading. Constant-stress-ratio tests do not distinguish between the flow- and deformation-type theories[1] and it was for this reason that emphasis in this report is placed on variable-stress-ratio tests. Constant-stress-ratio tests are also reported in order to provide basic information on the strength properties of the material tested. The present investigation is restricted to a 75S-T6 aluminum alloy subjected to biaxial tensile stresses only.

The research herein reported was conducted in the Plasticity Laboratory of the Pennsylvania State College under the sponsorship and with the financial assistance of the National Advisory Committee for Aeronautics. Dr. Sam Batdorf and his associates at Langley Field gave valued suggestions in the planning of the research reported herein. Messrs. B. H. Ulrich, W. P. Hughes, and L. W. Hu, research assistants, conducted the tests and computed the test data. Parts of the testing machine and the special strain gage were built by Messrs. S. S. Eckley, H. Johnson, and I. Bjalme. The assistance given by the NACA and the foregoing individuals in making possible this investigation is greatly appreciated.

SYMBOLS

d	original internal diameter of tubular specimen, inches
d_p	internal diameter of tubular specimen in plastic range, inches

[1] In this report, when reference is made to the flow and deformation theories, the simple theories based on the octahedral shear stress and strain are intended.

E	Young's modulus of elasticity, psi
e_1, e_2	longitudinal and lateral nominal strains in plastic range, respectively, inches per inch
k	strength coefficient for simple tension
μ	Poisson's ratio
n	strain-hardening coefficient for simple tension
p	internal pressure, psi
P	axial tension load, pounds
t	original wall thickness of tubular specimen, inches
t_p	wall thickness of tubular specimen in plastic range, inches
x, y	principal stress ratios
σ	true stress in simple tension, psi
σ_y	yield stress in simple tension, psi
σ_u	nominal ultimate stress in longitudinal tension, psi
σ_r	true rupture stress in longitudinal tension, psi
σ_1, σ_2	true longitudinal and lateral principal stresses, respectively, psi
σ_3	true radial principal stresses, psi
σ_{1e}, σ_{2e}	elastic longitudinal and lateral principal stresses, respectively, psi
σ_{1y}, σ_{2y}	yield longitudinal and lateral principal stresses, respectively, psi
σ_{1u}, σ_{2u}	nominal ultimate longitudinal and lateral principal stresses, respectively, psi
σ_{1r}, σ_{2r}	true longitudinal and lateral principal stresses at rupture, respectively, psi

$\bar{\sigma}$	significant stress, psi
ϵ	true strain in simple tension, inches per inch
$\epsilon_1, \epsilon_2, \epsilon_3$	true principal strains, inches per inch
$\bar{\epsilon}$	significant strain, inches per inch
$\epsilon_1', \epsilon_2', \epsilon_3'$	total principal strains, inches per inch
δB	increment in plastic flow $(F(\bar{\sigma})\delta\bar{\sigma})$

TEST PROCEDURE

Material Tested and Specimen

The material tested in this investigation was a fully heat-treated aluminum alloy designated as 75S-T6. The material was supplied in tubular extruded form in lengths of 16 feet with an internal diameter of 2 inches and a wall thickness of 1/4 inch. The nominal chemical composition, in addition to aluminum and normal impurities, consists of 1.6 percent copper, 2.5 percent magnesium, and traces of manganese and chromium. Nominal mechanical properties in tension as furnished by the manufacturer are: Ultimate strength, 88,000 psi; yield strength (0.2 percent offset), 80,000 psi; modulus of elasticity, 10.6×10^6 psi; percent elongation in 2 inches, 10 percent; and Poisson's ratio, 0.33.

The dimensions of the machined specimens are shown in figure 5 of reference 1. The specimen used had an over-all length of 16 inches, with an intermediate length of 11 inches of reduced wall thickness equal to about 0.100 ± 0.002 inches. The internal surface was left in the extruded form. The wall thickness of the tubular specimen was measured using the apparatus described in reference 1. The ratio of the wall thickness to diameter of the specimen was 0.05, so that the biaxial stresses throughout the wall were essentially constant. The ratio of diameter to length for the specimen was about 0.18, so that a sufficiently long section of the specimen was available free from bending stresses produced by end restraints.

Testing Machine

The machine used for the tests reported in reference 1 was modified for the present investigation. Changes in methods of applying the internal pressure and axial loads and a new-type clip gage were necessary in the present investigation to obtain more accurately the stress-strain relations for the initial part of the plastic range. Figure 1 shows front and side views of the biaxial-stress machine. The axial tensile load is applied to the specimen S by means of a hydraulic jack J, a vertical rod R, and a lever L. The axial load is measured by a dynamometer D using SR-4 gages. The lever L transmits the load to the specimen through spherical seats S' to insure axiality of loading. The fulcrum F of the lever and the ends of the lever are supplied with bearings to eliminate errors due to friction. The pulling rod R is provided with a spherical seat and a bearing to eliminate bending. A pump unit P was used to apply the internal pressure. A 10 W automotive oil with 175 SSU viscosity at 100° F was the fluid used for applying the internal pressure. The oil was supplied to the specimen S by a pump P through a high-pressure pipe line to the lower pulling head H. The rate of pressure application was controlled by means of a release valve V which discharged surplus oil into the oil-supply reservoir. The oil pressure was measured by a 10,000-pound U. S. Bourdon gage G.

The axiality of the load was checked as described in reference 1. The machine was calibrated for axial loading by using a calibrating rod with SR-4 gages in place of the specimen S and recording the readings on a calibrated mechanical type dynamometer at D. The axial load on the specimen could be measured within 100 pounds. The pressure gage was calibrated before testing and was found to have a maximum error of about 2 percent.

Method of Measuring Strains

The elastic strains were measured for a 13/16-inch gage length by using SR-4 electric strain gages. Two SR-4 gages, one longitudinal and one lateral, were attached to the specimen at midlength and were used to measure the elastic strains (fig. 2(a)). The SR-4 gages were cemented to the specimens in compliance with the procedure prescribed by the manufacturer. The strain gages were connected through a switch box B so that each gage could be successively switched into the circuit with the strain indicator I. The strain indicator I records the strain directly in microinches per inch.

The foregoing method of measuring strains is limited to a maximum strain value of about 0.015 inch per inch. In order to measure the plastic strains it was necessary to provide some other kind of strain gage. A clip-type gage as shown in figures 2 and 3 was used to measure

the longitudinal and lateral plastic strains. A clip gage consists of a rectangular-shaped frame with the cross member made of a phosphor-bronze strip to which SR-4 electric gages are attached to the upper and lower surfaces. By this arrangement, an additional temperature-compensating gage is not required and increased sensitivity is obtained. By means of these clip gages a large strain at the pivot points of the clip is reduced to a small measurable strain at the bridge of the clip. The longitudinal and lateral clip gages measure strains to 0.00005 inch per inch. The clip gage in figure 2 made it possible to measure both the longitudinal and lateral plastic strains on two gage lengths. The gages were calibrated using the device shown in figure 2(b). A stepped plate C with notches along the edges of the plate spaced at fixed known distances provides the standard for calibrating the clip gages. The distances between the notches were accurately measured by micrometer calipers reading to 0.0001 inch. With the clip gage attached to a pair of notches, the SR-4 indicator reading is recorded. By use of the successive notches and by observing the corresponding SR-4 indicator readings, a calibration of the clip gages is made possible.

Final strains at rupture were measured to 0.01 inch by use of dividers and a scale.

Method of Testing

Prior to testing, SR-4 gages were glued to a tubular specimen. After adjusting the clip gages and connecting all strain gages to the switching box and strain indicator, a zero set of strain readings on the unloaded specimen was recorded. Oil was then pumped through the specimen to remove any air that might be trapped in the specimen. The discharge outlet in the pulling head of the testing machine was then sealed and a protection shield was placed around the specimen. Internal pressure or axial loads or both types of loading were then applied according to predetermined values. The manner and magnitude of the loads applied naturally depended upon the specific type of test. At selected intervals of load or strain the values of the loads and strains were recorded. Fracture loads were noted and permanent strains after fracture were measured.

Prior to testing, all specimens were subjected to a permanent prestrain of 0.2 percent, first in the longitudinal direction and then in the lateral direction. This procedure was recommended by the NACA committee for this project. The purpose of the prestraining is to reduce the amount of anisotropy present in the extruded tubular specimen. Influence of such prestraining is described in a paper by Templin (reference 2).

CONSTANT-STRESS-RATIO TESTS

Plastic stress-strain relations for various constant biaxial stress ratios are the usual type obtained. To provide this standard information and to obtain control data, constant-stress-ratio tests were also conducted as part of the present investigation. It should be noted that constant-stress-ratio tests give also information on the influence of the combined stress ratio upon the strength and ductility of the material.

Conventional Stress-Strain Results

The average curve showing the relations between the conventional stress and strain for both the longitudinal and lateral stresses is shown in figures 4 and 5. On each stress-strain curve the ratio σ_2/σ_1 of the lateral to longitudinal stress is given. The strain values plotted in figures 4 and 5 were measured by the SR-4 gages cemented to the specimens. For most stress ratios three specimens were used, but for all ratios at least two specimens were tested.

The equations used for calculating the nominal longitudinal and lateral stresses plotted in figures 4 and 5 were, respectively,

$$\sigma_{1e} = \frac{pd^2 + 4\frac{P}{\pi}}{4t(d + t)} \tag{1}$$

$$\sigma_{2e} = \frac{pd}{2t}\left[\frac{1 + 2\frac{t}{d} + 2\left(\frac{t}{d}\right)^2}{1 + \frac{t}{d}}\right] \tag{2}$$

(see reference 1). Equation (2) for the lateral stress is that based on assuming that the wall thickness is large. It was necessary to consider the lateral stress based on the theory of the thick-wall tube since, for the value $t/d = 0.05$ used, $\sigma_{2e} = 1.05\frac{pd}{2t}$ minus a value 5 percent greater than that obtained by considering the theory of the thin-walled tube.

The nominal or conventional strain values plotted in figures 4 and 5 were determined from the values of the SR-4 indicator reading. The indicator readings were corrected for lateral sensitivity and the "combined-stress effect" since the manufacturer's constants are based

on a calibration using a steel specimen with a Poisson's ratio of 0.285. Equations for obtaining the corrected strain using the indicator readings are given in appendix B of reference 1.

Yield-strength values for axial tension (as given in table 1 for stress ratio equal to 0) were based on offset strain of 0.002 inch per inch, as shown in figure 4. For the combined-stress tests an equivalent offset strain was used. The determination of this equivalent offset strain is explained in appendix B.

Plastic Stress-Strain Results

The relation between the true stresses and strains for the entire range of stress and for the various principal stress ratios are given in figures 6 and 7. These stress-strain relations differ from the conventional diagrams since they consider a changing gage length and changing dimensions of the specimen. The curves shown in figures 6 and 7 are based on the average nominal stress-strain relation for at least two specimens.

The true plastic strains were determined from the clip-gage readings given by the SR-4 indicator. The conversion of the reading to strain in inches per inch is explained in reference 1.

It can be shown (reference 1) that the true longitudinal and lateral strains in terms of the nominal longitudinal and lateral strains e_1 and e_2 are

$$\left.\begin{aligned} \epsilon_1 &= \log_e (1 + e_1) \\ \epsilon_2 &= \log_e (1 + e_2) \end{aligned}\right\} \tag{3}$$

The stresses in the plastic range must be determined using the dimensions at the particular load values, since the changes in dimensions during plastic flow are appreciable. The true longitudinal and lateral stresses can be obtained by equations (1) and (2) provided the initial diameter d and wall thickness t are replaced by their actual values d_p and t_p at the particular loads considered. That is, the stresses in the plastic range are

$$\sigma_1 + \frac{p d_p^2 + 4 \frac{P}{\pi}}{4 t_p (d_p + t_p)} \tag{4}$$

$$\sigma_2 = \frac{pd_p}{2t_p} \tag{5}$$

The values of the dimensions d_p and t_p can be shown to be

$$t_p = \frac{t}{(1 + e_1 + e_2)} \tag{6}$$

$$d_p = (d + 2t)(1 + e_2) - 2t_p \tag{7}$$

The true stress-strain diagrams represented in figures 6 and 7 are based on stresses and strains as calculated by equations (3), (4), and (5). The fracture points shown in figures 6 and 7 were based on the strains after rupture corrected for the elastic strains just prior to rupture.

From the data given in figures 4 and 5, values of the nominal ultimate strengths for the various biaxial stress ratios were determined. These values are listed in table 2. Table 3 shows the true fracture stresses for various biaxial stress ratios, as determined from figures 6 and 7. Table 4 gives ductility values by listing the nominal and true strains at fracture for various biaxial stress ratios.

Analysis and Discussion

Yield strength.- Yield-strength values for various biaxial stress ratios (appendix B) are compared with the theoretical values in figure 8 and table 1. The comparison shown in figure 8 is based upon the uniaxial strength in the longitudinal direction. Figure 8 shows that the maximum-shear or stress theories are in approximate agreement with the test results.

Plastic stress-strain relations.- Plastic stress-strain relations are compared with the deformation theory by plotting relations between the significant stress and strain (reference 1) and comparing these relations with the true uniaxial stress-strain relations (figs. 9 and 10). The values of the significant stress and strain were computed by the equations

$$\bar{\sigma} = \sqrt{\frac{1}{2}\left[(\sigma_1 - \sigma_2)^2 + (\sigma_2 - \sigma_3)^2 + (\sigma_1 - \sigma_3)^2\right]} \tag{8}$$

$$\bar{\epsilon} = \sqrt{\frac{4}{3}\left(\epsilon_1^2 + \epsilon_1\epsilon_2 + \epsilon_2^2\right)} \tag{9}$$

Values of $\bar{\sigma}$ and $\bar{\epsilon}$ are also referred to as the "effective stress and strain" and they are equivalent to the "octahedral shear stress and strain" except for a numerical constant. A study of figure 10 shows that the deformation or flow theories can be used to approximately predict plastic stress-strain relations. This conclusion is based on the agreement between the various significant stress-strain relations and the true uniaxial stress-strain relation as shown in figure 10.

A comparison of the true stress-strain relations for each principal stress and the values predicted by the flow and deformation theories is given in figures 6 and 7. The determination of the theoretical stress-strain relations by the flow and deformation theories is explained in appendix A. For constant stress ratios the flow and deformation theories coincide. For small strains the two theories give the same results within the possible accuracy of the calculations. Figure 10 shows that there is good agreement between the actual stress-strain relations and the values predicted by both the flow and the deformation theories.

Biaxial nominal ultimate strength.- Values of biaxial nominal ultimate strength as given in table 2 are compared in figure 11 with values predicted by the maximum-stress or shear theory of failure. Figure 11 shows that the maximum-stress or shear theories may be used to approximately predict the nominal ultimate biaxial tensile strengths for Alcoa 75S-T6 aluminum alloy.

Biaxial true fracture strength.- Values of biaxial true fracture strength as listed in table 3 are compared in figure 12 with values given by the maximum-stress theory. An examination of figure 12 shows the maximum-stress or shear theories give an approximate prediction of fracture strength. In view of the necking down of the specimen beyond the ultimate loads and the subsequent changes in the state of stress due to necking, the comparison between theories and test results is considered better than might be expected.

Ductility.- Ductility values based upon both the initial and changing gage lengths are given in table 4 for various biaxial stresses. Both the nominal and true ductility values in table 4 show that the ductility decreases with increase in biaxiality of the principal stress ratio σ_2/σ_1 from 0 to 1. The influence of biaxial stresses on the ductility cannot be definitely determined because of the effect of anisotropy of the material. The initial prestressing of the material did not have the desired influence on the anisotropy of the material. The directional effects in the specimen are also indicated by the

difference in the true tensile stress-strain diagrams for the longitudinal and lateral directions as shown in figure 13. The difference in the tensile properties in the two directions is also shown by the difference in values of k and n as obtained from figure 13 and listed in table 5. Values of k and n are, respectively, the strength coefficient and strain-hardening exponent in the equation $\sigma = k\epsilon^n$, where σ and ϵ are the true tensile stress and strain, respectively.

VARIABLE-STRESS-RATIO TESTS

The constant-stress-ratio tests discussed in the foregoing section do not make it possible to distinguish between the flow and deformation theories since for constant biaxial stress ratios the theories coincide. Variable-stress-ratio tests were conducted in this investigation in an attempt to show which of the two theories agreed best with the test results.

Variable-stress-ratio tests were conducted in essentially the same manner as the constant-stress-ratio tests, except that the internal pressure was first applied up to selected values and axial tensile loads were then applied to fracture. The value of the internal pressure was maintained in each case while the axial load was applied. The manner of loading is indicated in figures 14 and 15 which show the nominal stress-strain relations for both the longitudinal and lateral stresses when various loading conditions were used. The nominal stresses used in plotting figures 14 and 15 were calculated by equations (1) and (2) and the strains were determined as explained in reference 1. Using equations (3), (4), and (5) and the average values represented by the curves in figures 14 and 15, the true stresses and strains were calculated and for each loading condition the values of true stress-strain relations were plotted for both the longitudinal and lateral directions. Figures 16 and 17 show these true stress-strain relations. Values of the true stress-strain relations as determined by the flow and deformation theories were computed as explained in appendix A. These values are based on the true tension stress-strain relations as previously noted. A comparison is shown in figure 16 between the test results and the values of the stress-strain relations predicted by the flow and deformation theories. An examination of figure 16 shows that both the flow and deformation theories are in approximate agreement with the test results and that one cannot be recommended in preference to the other.

To compare the deformation theory and test results, significant stress-strain relations were plotted for the variable-stress-ratio tests as shown in figure 18. Figure 19 shows the significant stress-strain

relations plotted with a common origin as well as the true uniaxial tensile stress-strain relation. An examination of the significant stress-strain curves in figure 10 for constant stress ratios indicates that some of the differences between the significant stress-strain relations in figure 19 are due to anisotropy. The anisotropy is shown by the difference between significant stress-strain relations in figure 10 for the uniaxial lateral and longitudinal stresses - that is, for principal stress ratios 0 and ∞.

SPECIAL TESTS

Tests on Isotropic Yielding

It is assumed in the isotropic linear flow theories that initial prestraining will not produce anisotropy. That is, it is assumed that there is isotropic yielding. To determine experimentally the validity of this assumption the following tests were made. One specimen was loaded in longitudinal uniaxial tension to a strain of about 5 percent. The specimen was unloaded and then loaded under uniaxial lateral tension to failure. A second specimen was loaded in longitudinal uniaxial tension to about 5-percent strain, unloaded, and then reloaded under uniaxial longitudinal tension to failure. If the isotropic-yielding assumption is valid the significant stress-strain curves for these two tests would coincide. A plot of the significant stress-strain relations showed that the curves were in about as close agreement as the significant stress-strain relations for longitudinal tension and lateral tension in figure 10. Furthermore, the lack of ductility in the lateral direction gave a small over-all range of strain, making the comparison of the significant stress-strain plots not entirely conclusive. That is, the initial anisotropy of the material made it difficult to determine whether isotropic yielding occurred.

Tests on Coincidence of Principal Stress and Strain Axes

In the theories of plasticity, it is assumed that the direction of the principal stresses and strains remains the same in the plastic range. To check this assumption, a strain rosette was placed on a tubular specimen in order to provide a means of determining the principal strain directions. The specimen was then subjected to an internal pressure and values of strains for the three strain-rosette directions were measured up to a strain of about 1.5 percent. The pressure was then removed and the permanent plastic strains were measured. From the strain-rosette readings the directions of the principal plastic strains were determined. A comparison of the directions of the principal plastic stresses and strains as shown in figure 20 shows that for practical purposes the direction of these axes coincide as assumed in the theory.

CONCLUSIONS

For the 75S-T6 aluminum alloy tested, the following conclusions are made on the basis of the foregoing biaxial tension tests:

1. The biaxial yield strengths may be safely predicted by the maximum-shear or stress theories.

2. The nominal biaxial ultimate strengths and the true biaxial fracture strengths are in approximate agreement with both the maximum-stress and maximum-shear theories. For all three kinds of strength, the lines defining the theories are not definitely fixed since the testing of more specimens for uniaxial stresses may have shifted the location of the lines defining the theories.

3. Although the test results indicate a decrease in ductility with biaxial tension compared with uniaxial tension, the ductility values may have been influenced by the anisotropy of the material.

4. For constant principal stress ratios, the octahedral deformation theory gives a good engineering approximation for defining the plastic biaxial stress-strain relations.

5. For the particular load path and principal stresses used the variable-stress test results show that both the deformation and flow theories give a good approximation to the actual stress-strain relations.

6. For large plastic strains, the assumption of isotropic yielding made in the plasticity theories is in general agreement with the test results.

7. For the tests of constant principal stress ratio it was shown that the principal axes of stress and strain coincide within the limits of possible experimental error. This conclusion indicates that any initial anisotropy of the material does not influence the theoretical values as given by the simple deformation or flow theories.

The Pennsylvania State College
State College, Pa., May 27, 1950

APPENDIX A

DETERMINATION OF THEORETICAL STRESS-STRAIN RELATIONS BY DEFORMATION AND FLOW THEORIES

In the interpretation of test results on plastic combined stress-strain relations, the deformation- and flow-type theories are usually based on distortion-energy or octahedral-shear-stress criterions of flow. The determination of the stress-strain relation based on the uniaxial simple-tension stress-strain relation for both theories will be outlined in the following sections.

Stress-Strain Relations by the Deformation Theory

On the basis of the assumptions that the sum of the principal plastic strains is zero and that the ratios of the principal shear stresses and strains are proportional, it can be shown (reference 1) that the principal plastic strains in terms of the principal stresses are

$$\left.\begin{aligned} \epsilon_1 &= \left(\frac{\epsilon}{\sigma}\right)\left[\sigma_1 - \frac{1}{2}\left(\sigma_2 + \sigma_3\right)\right] \\ \epsilon_2 &= \left(\frac{\epsilon}{\sigma}\right)\left[\sigma_2 - \frac{1}{2}\left(\sigma_1 + \sigma_3\right)\right] \\ \epsilon_3 &= \left(\frac{\epsilon}{\sigma}\right)\left[\sigma_3 - \frac{1}{2}\left(\sigma_1 + \sigma_2\right)\right] \end{aligned}\right\} \tag{A1}$$

In equations (A1), σ and ϵ are the true stress and plastic strain for simple tension.

Squaring both sides of equations (A1) and adding the resulting equations yield

$$\frac{\epsilon}{\sigma} = \frac{\bar{\epsilon}}{\bar{\sigma}} \tag{A2}$$

where

$$\bar{\epsilon} = \sqrt{\frac{2}{3}\left(\epsilon_1^2 + \epsilon_2^2 + \epsilon_3^2\right)} \tag{A3}$$

and

$$\bar{\sigma} = \frac{1}{\sqrt{2}}\sqrt{\left(\sigma_1 - \sigma_2\right)^2 + \left(\sigma_2 - \sigma_3\right)^2 + \left(\sigma_3 - \sigma_1\right)^2} \tag{A4}$$

and $\bar{\sigma}$ and $\bar{\epsilon}$ are called the significant or effective stress and strain.

It is now possible by means of equations (A1), (A2), (A3), and (A4) and the simple-tension stress-strain curve to obtain the principal plastic strains. That is:

(1) For given values of the principal stresses σ_1, σ_2, and σ_3, the value of the significant stress $\bar{\sigma}$ can be determined by equation (A4)

(2) From the simple-tension stress-plastic-strain relation using the value of $\sigma = \bar{\sigma}$ obtained in step 1, corresponding values of $\epsilon = \bar{\epsilon}$ are found

(3) With $\bar{\epsilon}$ and $\bar{\sigma}$ known, for given values of the principal stresses equations (A1) can be used to determine the plastic strains ϵ_1, ϵ_2, and ϵ_3

(4) For other values of the principal stresses, the above steps may be repeated

To obtain the predicted stress-strain curves for each of the principal stresses, it is first necessary to add the plastic strain values to the elastic in order to obtain the total strains. That is, the total strains are

$$\left.\begin{aligned}
\epsilon_1' &= \frac{1}{E}\left[\sigma_1 - \mu\left(\sigma_2 + \sigma_3\right)\right] + \epsilon_1 \\
\epsilon_2' &= \frac{1}{E}\left[\sigma_2 - \mu\left(\sigma_1 + \sigma_3\right)\right] + \epsilon_2 \\
\epsilon_3' &= \frac{1}{E}\left[\sigma_3 - \mu\left(\sigma_2 + \sigma_1\right)\right] + \epsilon_3
\end{aligned}\right\} \tag{A5}$$

By equations (A5) the total principal strains ϵ_1', ϵ_2', and ϵ_3' can be determined and the theoretical stress-strain relations based on the deformation theory plotted. In figures 6, 7, 16, and 17 stress-strain relations based on the foregoing procedure are shown.

Stress-Strain Relations by the Flow Theory

The flow-type theory for predicting plastic stress-strain relations differs from the deformation-type theory by assuming that the incremental changes in principal shear stresses are proportional to the incremental changes in the principal shear strains. The procedure developed in the following discussion for the tube subjected to internal pressure and axial tension is adapted from the general theory given by Shepherd in reference 3.

When increments of principal shear stress and strain are assumed to be proportional, then equations (A5) are replaced by increments of strains or

$$\left.\begin{aligned}
\delta\epsilon_1' &= \frac{1}{E}\left[\delta\sigma_1 - \mu\left(\delta\sigma_2 + \delta\sigma_3\right)\right] + \delta\epsilon_1 \\
\delta\epsilon_2' &= \frac{1}{E}\left[\delta\sigma_2 - \mu\left(\delta\sigma_1 + \delta\sigma_3\right)\right] + \delta\epsilon_2 \\
\delta\epsilon_3' &= \frac{1}{E}\left[\delta\sigma_3 - \mu\left(\delta\sigma_2 + \delta\sigma_1\right)\right] + \delta\epsilon_3
\end{aligned}\right\} \tag{A6}$$

where the increments of plastic strain are

$$\left.\begin{aligned}
\delta\epsilon_1 &= \delta B\left[\sigma_1 - \frac{1}{2}\left(\sigma_2 + \sigma_3\right)\right] \\
\delta\epsilon_2 &= \delta B\left[\sigma_2 - \frac{1}{2}\left(\sigma_3 + \sigma_1\right)\right] \\
\delta\epsilon_3 &= \delta B\left[\sigma_3 - \frac{1}{2}\left(\sigma_1 + \sigma_2\right)\right]
\end{aligned}\right\} \tag{A7}$$

From equations (A6) and (A7) the total-strain increments, equal to the sum of the elastic and plastic strain increments, become

$$\left.\begin{aligned}
\delta\epsilon_1' &= \frac{1}{E}\left[\delta\sigma_1 - \mu\left(\delta\sigma_2 + \delta\sigma_3\right)\right] + \delta B\left[\sigma_1 - \frac{1}{2}\left(\sigma_2 + \sigma_3\right)\right] \\
\delta\epsilon_2' &= \frac{1}{E}\left[\delta\sigma_2 - \mu\left(\delta\sigma_3 + \delta\sigma_1\right)\right] + \delta B\left[\sigma_2 - \frac{1}{2}\left(\sigma_3 + \sigma_1\right)\right] \\
\delta\epsilon_3' &= \frac{1}{E}\left[\delta\sigma_3 - \mu\left(\delta\sigma_1 + \delta\sigma_2\right)\right] + \delta B\left[\sigma_3 - \frac{1}{2}\left(\sigma_1 + \sigma_2\right)\right]
\end{aligned}\right\} \qquad (A8)$$

The beginning of plastic flow is defined by the distortion-energy theory or the equivalent octahedral shear stress. That is, if σ_y is the yield stress in simple tension the relation between the stress components for plastic flow is

$$\sigma_y^2 = \sigma_1^2 + \sigma_2^2 + \sigma_3^2 - \sigma_1\sigma_2 - \sigma_2\sigma_3 - \sigma_3\sigma_1 \qquad (A9)$$

It is then assumed that the function given by equation (A9) which defines beginning of plastic flow is a function defining the subsequent plastic flow. That is, δB in equations (A7) and (A8) is assumed to to be a function $F(\overline{\sigma})\,\delta\overline{\sigma}$ of $\overline{\sigma}$ where $\overline{\sigma}$ is defined by

$$\overline{\sigma}^2 = \sigma_1^2 + \sigma_2^2 + \sigma_3^2 - \sigma_1\sigma_2 - \sigma_2\sigma_3 - \sigma_3\sigma_1 \qquad (A10)$$

It will be assumed furthermore that: (1) For $\delta\overline{\sigma} < 0$,

$$\delta B = 0 \qquad (A11)$$

and the increment of strain is elastic. (2) For $\delta\overline{\sigma} > 0$,

$$\delta B = F(\overline{\sigma})\delta\overline{\sigma} \qquad (A12)$$

and the increment of strain is elastic and plastic. To determine the principal stress-strain relations, it is necessary to determine the increment of strains from equations (A8). To obtain these strain increments the values of δB must be known for a given set of stresses. To determine δB equations (A10) and (A12) will be used, together with the simple-tension stress-strain diagram. For simple tension, by equations (A8), since $\sigma_1 = \sigma$ and $\sigma_2 = \sigma_3 = 0$,

$$\delta\epsilon' - \frac{1}{E}\,\delta\sigma = \delta B\sigma \qquad (A13)$$

By equation (A10) for simple tension $\sigma_1 = \sigma$, $\sigma_2 = \sigma_3 = 0$, and $\bar{\sigma} = \sigma$, and equation (A13) can be written as

$$\delta\epsilon' - \frac{1}{E}\delta\sigma = \bar{\sigma}\delta B \tag{A14}$$

Substituting the value of δB from equation (A12) in equation (A14),

$$\left(\delta\epsilon' - \frac{1}{E}\delta\sigma\right) = \bar{\sigma}F(\bar{\sigma})\delta\bar{\sigma} \tag{A15}$$

For a finite amount of straining by summing up the strains,

$$\left(\epsilon' - \frac{\sigma}{E}\right) = \sum \bar{\sigma}F(\bar{\sigma})\delta\bar{\sigma} \tag{A16}$$

Since the left-hand side of equation (A16) represents the plastic strain ϵ, by equation (A16)

$$\epsilon = \sum \bar{\sigma}F(\bar{\sigma})\delta\bar{\sigma} \tag{A17}$$

From the tension test curve, values of $\epsilon = \epsilon' - \sigma/E$ can be obtained for given values of $\sigma = \bar{\sigma}$. Since by equation (A17) $\epsilon = \sum \bar{\sigma}F(\bar{\sigma})\delta\bar{\sigma}$, a graph can be plotted showing the relation between $\sum \bar{\sigma}F(\bar{\sigma})\delta\bar{\sigma}$ and $\bar{\sigma}$. From this graph and by graphical integration values of $\bar{\sigma}F(\bar{\sigma})$ can be obtained for each value of $\bar{\sigma}$. Then, dividing $\bar{\sigma}F(\bar{\sigma})$ values by the corresponding $\bar{\sigma}$ values, the $F(\bar{\sigma})$ can be determined for each $\bar{\sigma}$ stress. It is then possible to plot a curve showing the relation between $F(\bar{\sigma})$ and $\bar{\sigma}$. With the relation between $F(\bar{\sigma})$ and $\bar{\sigma}$ known from the tension test results, it is now possible to obtain the theoretical stress-strain relations for the tube subjected to internal pressure and axial loading. To do this, the following steps are involved:

(1) For various values of σ_1 the values of $\bar{\sigma}$ are determined by equation (A10) listed in a table containing the following headings:

σ_1	$\bar{\sigma}$	$F(\bar{\sigma})$	$F(\bar{\sigma})\left(\sigma_1 - \frac{\sigma_2}{2}\right)$	$\sum F(\bar{\sigma})\left(\sigma_1 - \frac{\sigma_2}{2}\right)\delta\bar{\sigma}$	$\sum F(\bar{\sigma})\delta\bar{\sigma} = \sum \delta B$

(2) From the $F(\bar{\sigma})$ - $\bar{\sigma}$ curve obtained by using the stress-strain curve for simple tension, values of $F(\bar{\sigma})$ can be found for each $\bar{\sigma}$ value and their magnitudes placed in the correct column above.

(3) The products $F(\bar{\sigma})\left(\sigma_1 - \frac{\sigma_2}{2} - \frac{\sigma_3}{2}\right)$ are then computed and listed in the table.

(4) The relation $F(\bar{\sigma})\left(\sigma_1 - \frac{\sigma_2}{2} - \frac{\sigma_3}{2}\right)$ is then plotted against $\bar{\sigma}$.

(5) From the plot obtained in step (4) the values $\sum F(\bar{\sigma})\left(\sigma_1 - \frac{\sigma_2}{2} - \frac{\sigma_3}{2}\right)$ can be obtained since these values are the areas under the curve for the particular value of $\bar{\sigma}$. These values are the plastic strains since by equations (A8) and (A12) the plastic strains

$$\begin{aligned}\epsilon_1 &= \sum \delta\epsilon_1 \\ &= \sum \delta B\left[\sigma_1 - \tfrac{1}{2}\left(\sigma_2 + \sigma_3\right)\right] \\ &= \sum F(\bar{\sigma})\left[\sigma_1 - \tfrac{1}{2}\left(\sigma_2 + \sigma_3\right)\right]\delta\bar{\sigma}\end{aligned}$$

(6) Then by adding the plastic strains from step (5) to the elastic strains, the total strains become

$$\left.\begin{aligned}\epsilon_1' &= \frac{1}{E}\left[\sigma_1 - \mu\left(\sigma_2 + \sigma_3\right)\right] + \sum \delta B\left[\sigma_1 - \tfrac{1}{2}\left(\sigma_2 + \sigma_3\right)\right] \\ \epsilon_2' &= \frac{1}{E}\left[\sigma_2 - \mu\left(\sigma_1 + \sigma_3\right)\right] + \sum \delta B\left[\sigma_2 - \tfrac{1}{2}\left(\sigma_1 + \sigma_3\right)\right] \\ \epsilon_3' &= \frac{1}{E}\left[\sigma_3 - \mu\left(\sigma_1 + \sigma_2\right)\right] + \sum \delta B\left[\sigma_3 - \tfrac{1}{2}\left(\sigma_1 + \sigma_2\right)\right]\end{aligned}\right\} \qquad \text{(A18)}$$

That is, by equations (A18) the theoretical principal stress-strain relations can be obtained. The curves designated by the flow theory in figures 6, 7, 16, and 17 were plotted using equations (A18) and the foregoing procedure.

APPENDIX B

DETERMINATION OF EQUIVALENT OFFSET STRAIN FOR DETERMINATION OF BIAXIAL YIELD STRESSES[1]

For materials with strain-hardening, it is common practice to determine the yield stress by the use of the offset method as illustrated in figure 4 for simple tension. For states of combined stresses the procedure for the determination of yield stresses has not been standardized and various methods have been used. The method developed in the following discussion for the determination of yield stress appears to be the most logical. In this method, the yield stress is based on an offset strain - an equivalent offset strain - a value which takes into account the influence of combined stresses and a value which is based on the offset strain used for simple tension. The determination of this equivalent offset strain is based on the deformation theory.

By the deformation theory, since $\sigma = \bar{\sigma}$, the principal strains ϵ_1 and ϵ_2 can be obtained in terms of the uniaxial strain ϵ and the principal stresses by substituting $\bar{\sigma}$ for σ as given by equation (A4) in equations (A1). That is,

$$\left.\begin{aligned} \epsilon_1 &= \frac{\epsilon(2 - R)}{2\sqrt{1 - R + R^2}} \\ \epsilon_2 &= \frac{\epsilon(2R - 1)}{2\sqrt{1 - R + R^2}} \end{aligned}\right\} \tag{B1}$$

where R is the principal stress ratio σ_2/σ_1.

For an offset plastic strain $\epsilon = \epsilon_o$, the equivalent offset principal strains ϵ_{1_o} and ϵ_{2_o} are, by equations (B1),

$$\left.\begin{aligned} \epsilon_{1_o} &= \frac{(2 - R)}{2\sqrt{1 - R + R^2}}\epsilon_o \\ \epsilon_{2_o} &= \frac{2R - 1}{2\sqrt{1 - R + R^2}}\epsilon_o \end{aligned}\right\} \tag{B2}$$

[1]This procedure was suggested by Mr. L. W. Hu, Research Assistant, The Pennsylvania State College.

For various values of the principal stress ratio $R = \sigma_2/\sigma_1$, equations (B2) define the equivalent offset strains as used in figures 4 and 5.

REFERENCES

1. Marin, Joseph, Faupel, J. H., Dutton, V. L., and Brossman, M. W.: Biaxial Plastic Stress-Strain Relations for 24S-T Aluminum Alloy. NACA TN 1536, 1948.

2. Templin, R. L., and Sturm, R. G.: Some Stress-Strain Studies of Metals. Jour. Aero. Sci., vol. 7, no. 5, March 1940, pp. 189-198.

3. Shepherd, W. M.: Plastic Stress-Strain Relations. Proc. Institution Mech. Eng., vol. 159, 1948, pp. 95-99, discussion, pp. 99-114. (Formerly War Emergency Issue No. 39.)

TABLE 1

YIELD STRESSES FOR VARIOUS RATIOS OF BIAXIAL STRESSES

Biaxial stress ratio, σ_2/σ_1	Longitudinal yield stress, σ_{1y} (psi)	Lateral yield stress, σ_{2y} (psi)	Stress ratios	
			$x = \frac{\sigma_{1y}}{\sigma_y}$	$y = \frac{\sigma_{2y}}{\sigma_y}$
0	67.5×10^3	----------	0.94	-----
	72.1	----------	1.00	-----
	76.6	----------	1.06	-----
	[a]72.0	----------	[a]1.00	-----
0.5	73.5	39.7×10^3	1.02	0.55
	74.5	38.0	1.04	.53
	[a]74.0	[a]38.8	[a]1.03	[a].54
1.0	72.5	70.5	1.01	0.98
	71.0	73.0	.98	1.01
	74.0	71.5	1.03	.99
	[a]72.5	[a]71.7	[a]1.01	[a].99
2.0	37.0	76.2	0.51	1.06
	38.0	76.0	.53	1.06
	[a]37.5	[a]76.1	[a].52	[a]1.06
∞	----------	68.6	-----	0.95
	----------	71.5	-----	.99
	----------	[a]70.1	-----	[a].97

[a]Average value.

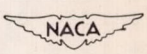

TABLE 2

NOMINAL ULTIMATE STRESSES FOR VARIOUS BIAXIAL STRESS RATIOS

Biaxial stress ratio, σ_2/σ_1	Specimen	Longitudinal nominal ultimate stress, σ_{1u} (psi)	Lateral nominal ultimate stress, σ_{2u} (psi)	Stress ratios	
				$x = \sigma_{1u}/\sigma_u$	$y = \sigma_{2u}/\sigma_u$
0 (Longitudinal tension)	21	85.7×10^3	0	1.04	0
	29	83.2	0	1.01	0
	34	78.6	0	.95	0
		[a]82.5	[a]0	[a]1.00	[a]0
0.5	A2	90.0	45.0×10^3	1.09	0.55
	A3	87.5	44.8	1.06	.54
	18	86.5	43.2	1.05	.52
		[a]88.0	[a]44.0	[a]1.07	[a].53
1.0	10	88.0	88.2	1.07	1.07
	11	77.4	77.5	.94	.94
	12	78.8	78.8	.96	.96
		[a]81.4	[a]81.5	[a].99	[a].99
2.0	37	40.4	80.4	0.49	0.98
	25	40.2	81.6	.49	.99
		[a]40.3	[a]81.0	[a].49	[a].98
∞ (Transverse tension)	38	0	72.5	0	0.88
	A1	0	73.1	0	.89
		[a]0	[a]72.8	[a]0	[a].88

[a]Average value.

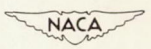

TABLE 3

TRUE FRACTURE STRESSES FOR VARIOUS BIAXIAL STRESS RATIOS

Biaxial stress ratio, σ_2/σ_1	Specimen	Longitudinal true fracture stress, σ_{1r} (psi)	Lateral true fracture stress, σ_{2r} (psi)	Stress ratios	
				$x = \sigma_{1r}/\sigma_r$	$y = \sigma_{2r}/\sigma_r$
0 (Longitudinal tension)	21	97.0×10^3	0	1.04	0
	29	94.2	0	1.01	0
	34	89.0	0	.95	0
		[a]93.4	[a]0	[a]1.00	[a]0
0.5	A2	95.8	48.1×10^3	1.03	0.52
	A3	93.2	47.7	1.00	.51
	18	92.1	45.2	.99	.49
		[a]93.7	[a]47.0	[a]1.01	[a].51
1.0	10	95.1	93.0	1.02	1.00
	11	83.6	81.6	.90	.88
	12	85.3	83.1	.92	.89
		[a]88.0	[a]85.9	[a].94	[a].92
2.0	37	41.2	80.6	0.44	0.86
	25	41.0	81.8	.44	.88
		[a]41.1	[a]81.2	[a].44	[a].87
∞ (Lateral tension)	38	0	73.7	0	0.79
	A1	0	74.4	0	.81
		[a]0	[a]74.0	[a]0	[a].80

[a]Average value.

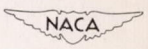

TABLE 4

NOMINAL AND TRUE DUCTILITY VALUES FOR VARIOUS BIAXIAL STRESS RATIOS

Biaxial stress ratio, σ_2/σ_1	Specimen	Nominal ductility (in./in.)	True ductility (in./in.)
0 (Longitudinal tension)	21	12.1×10^{-2}	11.3×10^{-2}
	29	13.5	12.6
	34	13.0	12.2
		[a]12.8	[a]12.0
0.5	A2	7.5	7.2
	A3	7.0	6.7
	18	6.0	5.8
		[a]7.0	[a]6.7
1.0	10	4.0	3.9
	11	3.0	3.1
	12	3.5	3.4
		[a]3.5	[a]3.5
2.0	37	2.0	1.9
	25	2.0	1.9
		[a]2.0	[a]1.9
∞ (Lateral tension)	38	2.5	2.1
	A1	1.5	1.3
		[a]2.0	[a]1.7

[a]Average value.

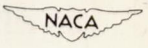

TABLE 5

TRUE STRESS-STRAIN RELATIONS FOR UNIAXIAL TENSION TESTS

Loading direction	Specimen	Nominal ultimate stress (psi)	True fracture stress (psi)	True ductility (in./in.)	Constant k (psi)	Constant n
Longitudinal	21	85.7×10^3	97.0×10^3	11.3×10^{-2}	----------	-----
	29	83.2	94.2	12.6	----------	-----
	34	78.6	89.0	12.2	----------	-----
		[a]82.5	[a]93.4	[a]12.0	[a]1.09×10^5	[a]0.08
Transverse	38	72.5	73.7	2.1	----------	-----
	A1	73.1	74.4	1.3	----------	-----
		[a]72.8	[a]74.0	[a]1.7	[a]0.88	[a]0.04

[a]Average value.

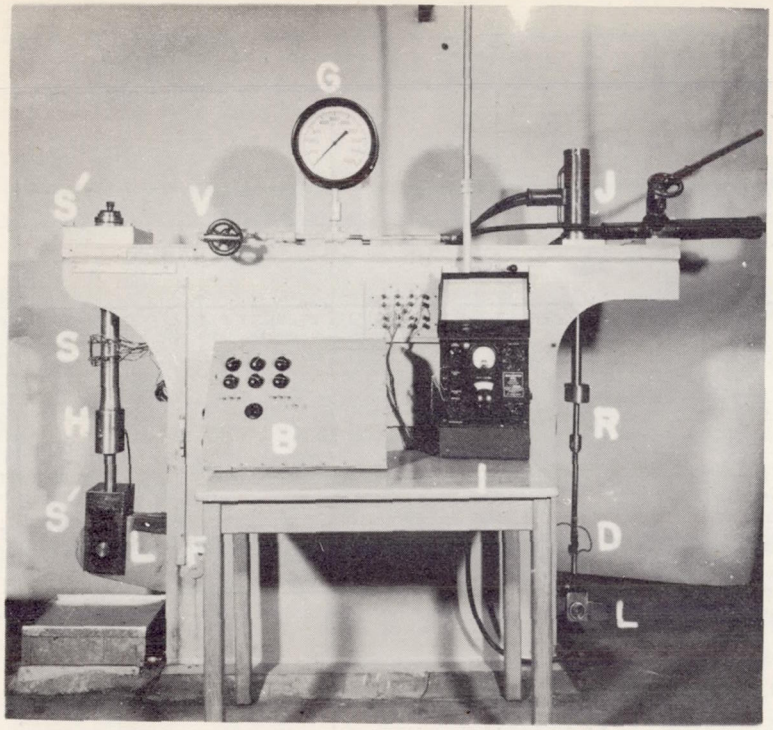

(a) Front view.

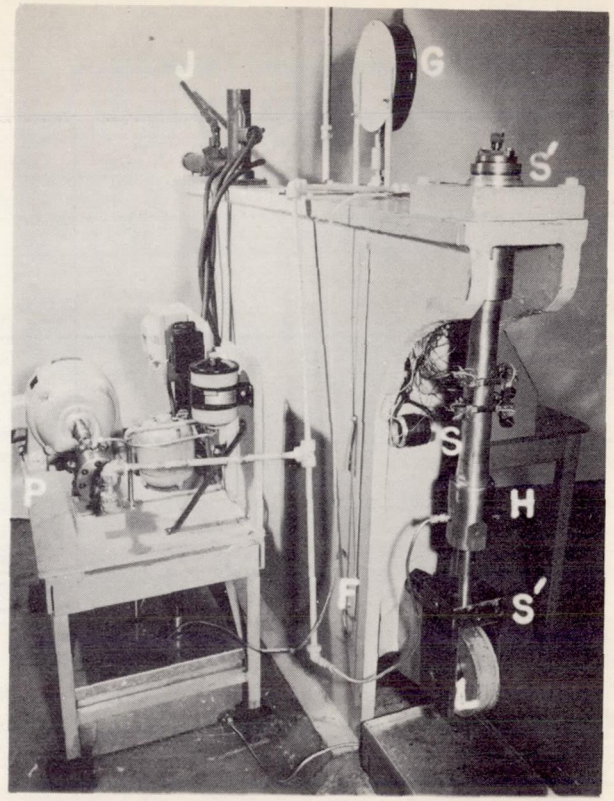

(b) Side view.

Figure 1.- Biaxial-stress testing machine.

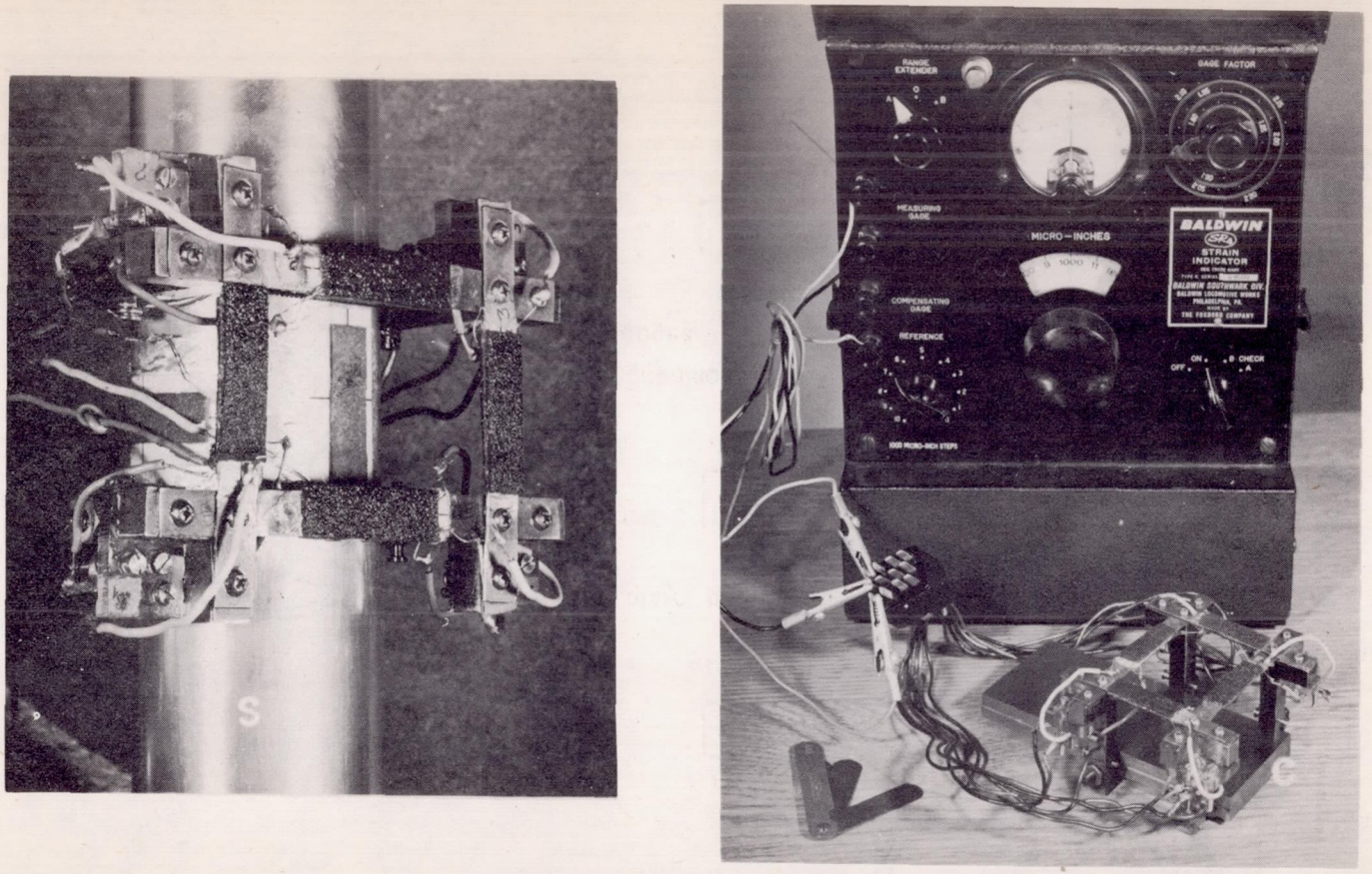

(a) Clip gage attached to specimen.

(b) Device for calibrating clip gage.

Figure 2.- Photograph of clip gage.

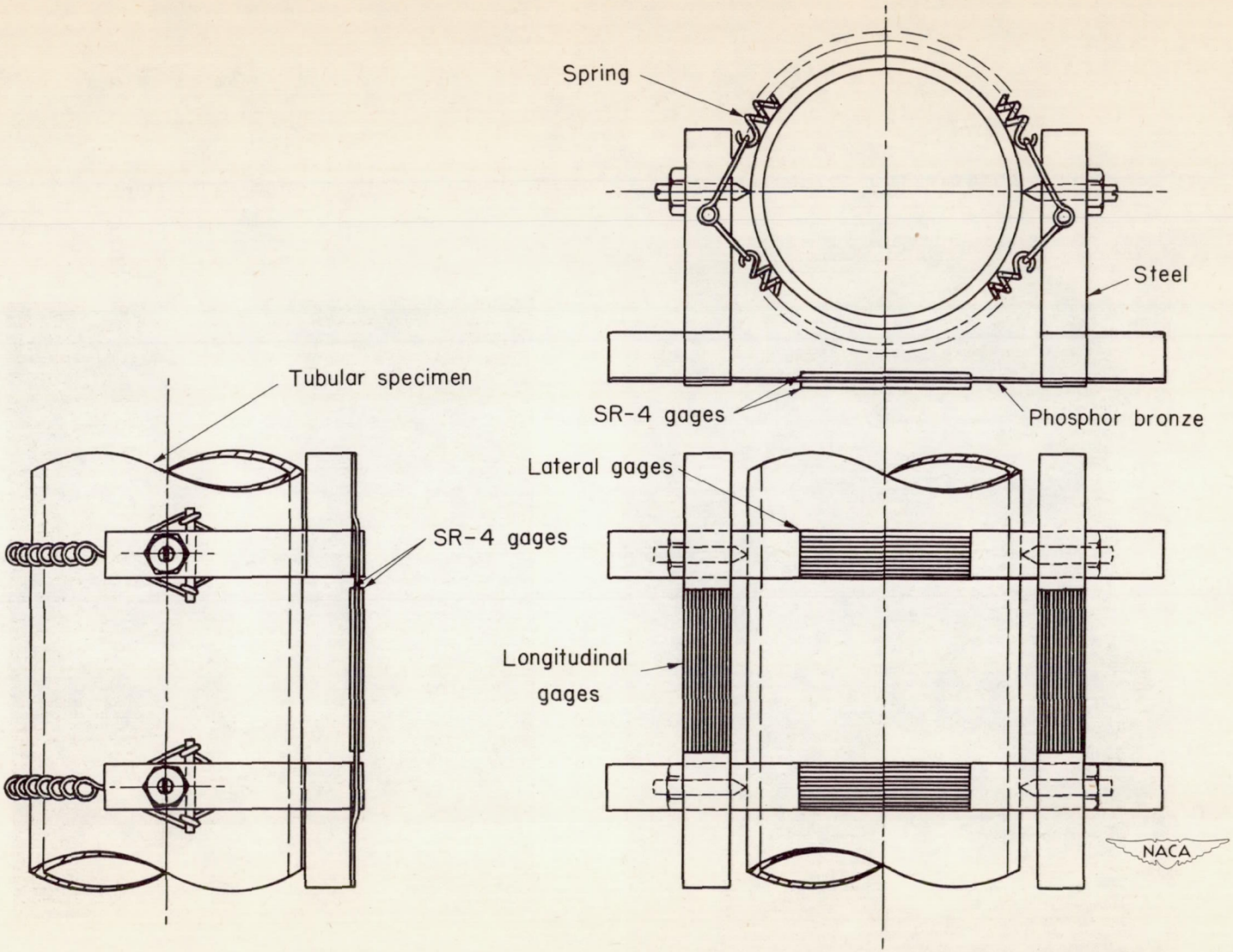

Figure 3.- Drawing of clip gage.

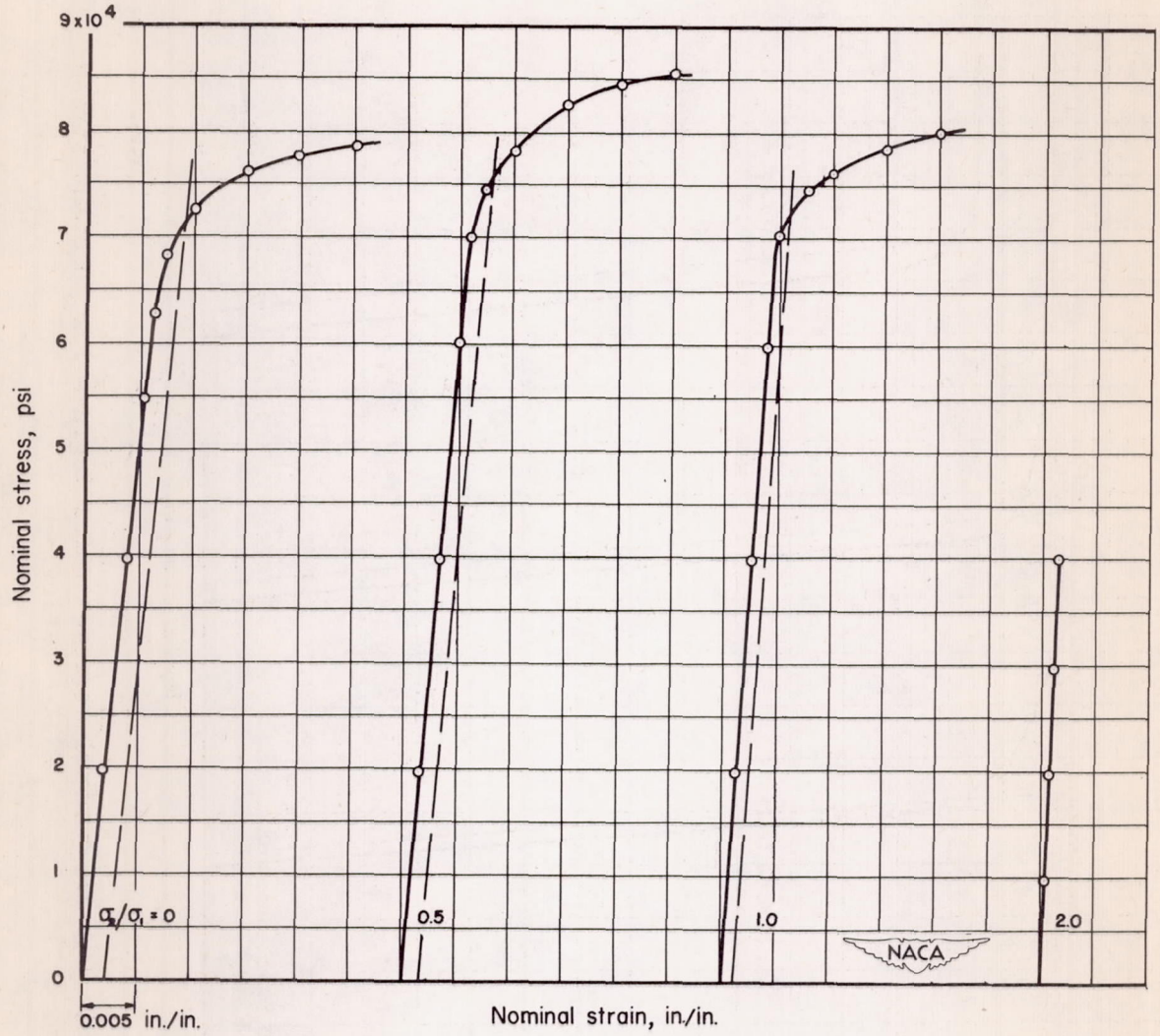

Figure 4.- Longitudinal nominal stress-strain diagrams for constant stress ratios.

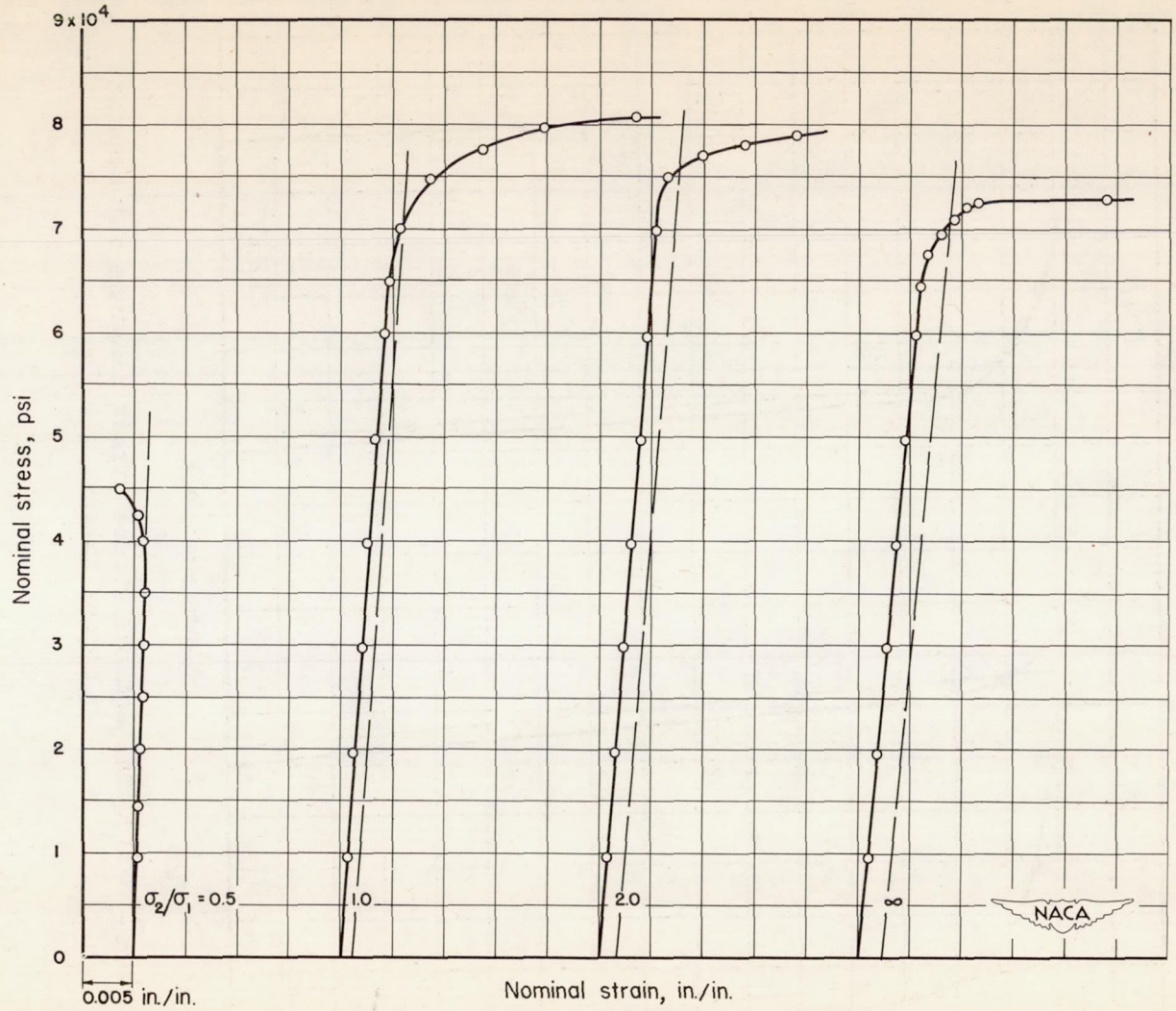

Figure 5.- Lateral nominal stress-strain diagrams for constant stress ratios.

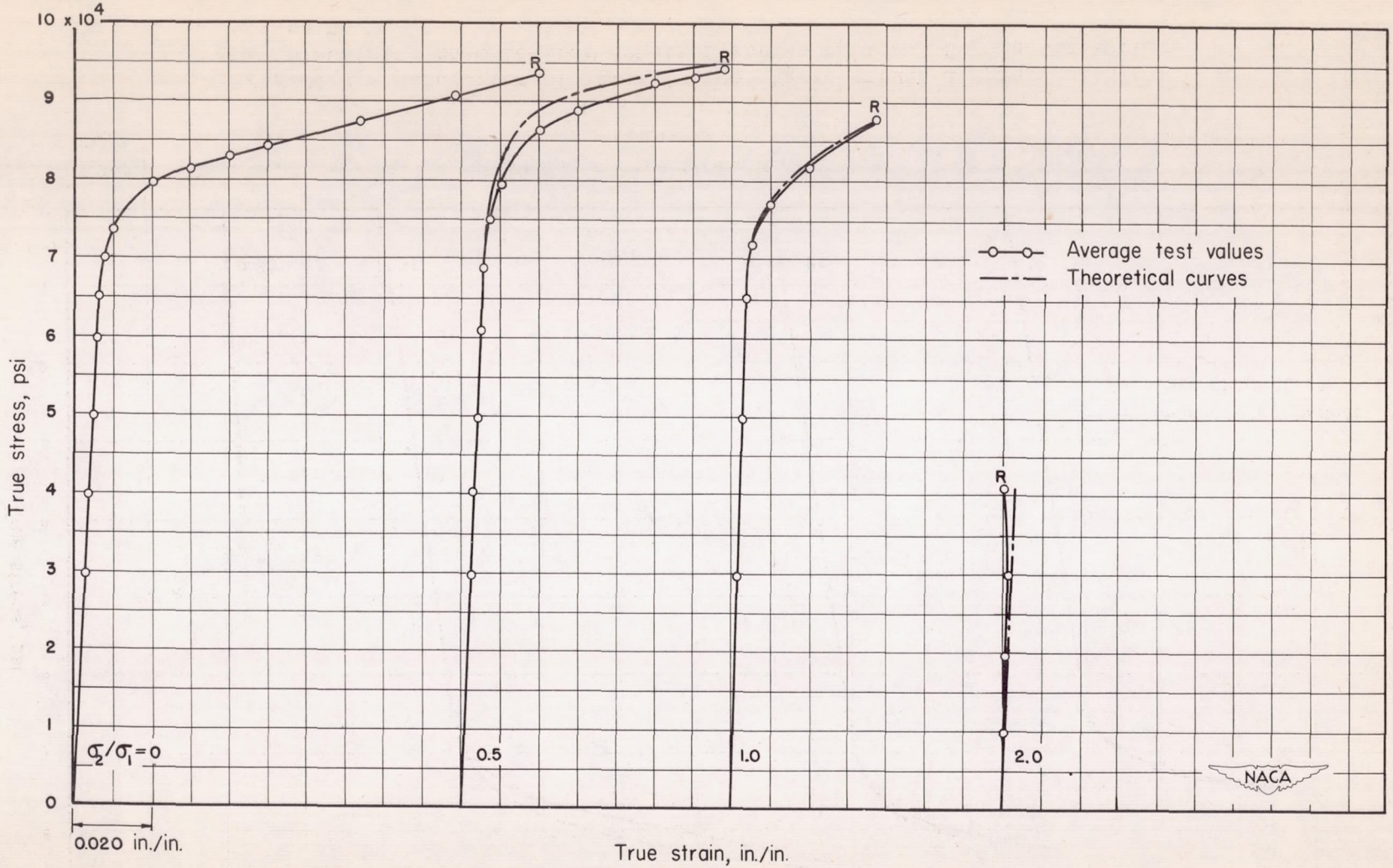

Figure 6.- Comparison of longitudinal true stress-strain diagrams with plasticity theories for constant stress ratios. R denotes rupture point.

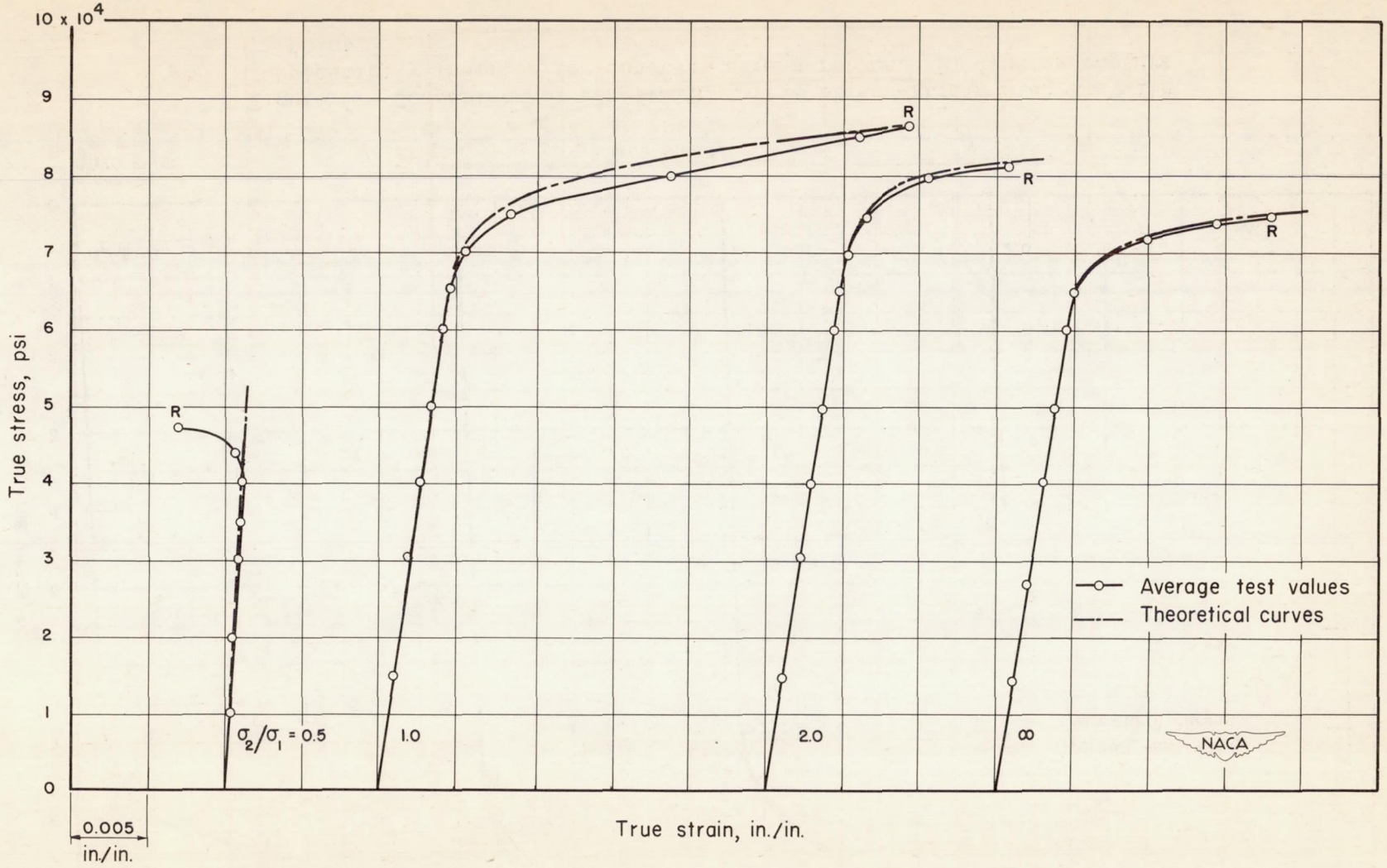

Figure 7.- Comparison of lateral true stress-strain diagrams with plasticity theories for constant stress ratios. R denotes rupture point.

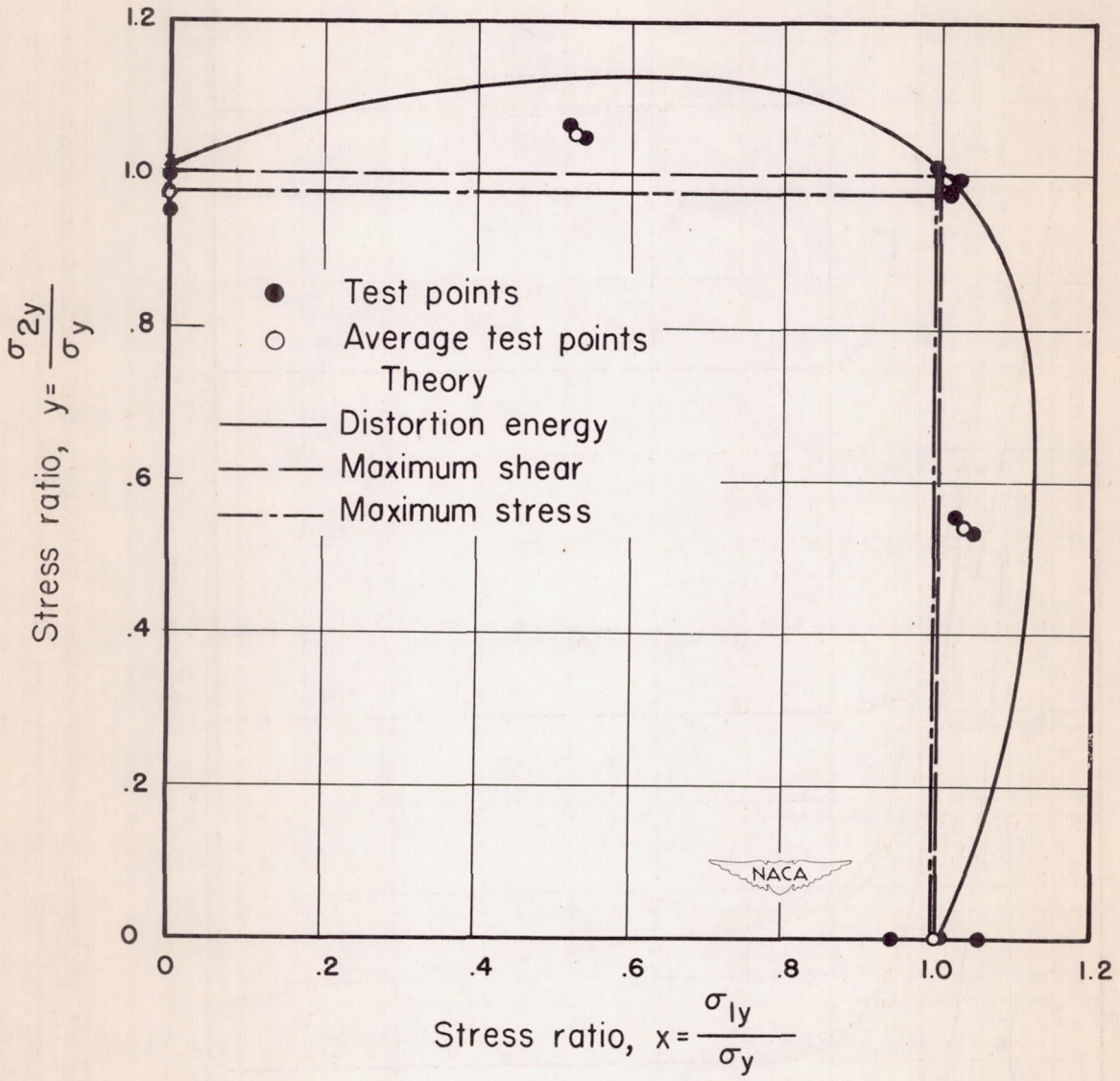

Figure 8.- Comparison of yield strengths with theories of failure.

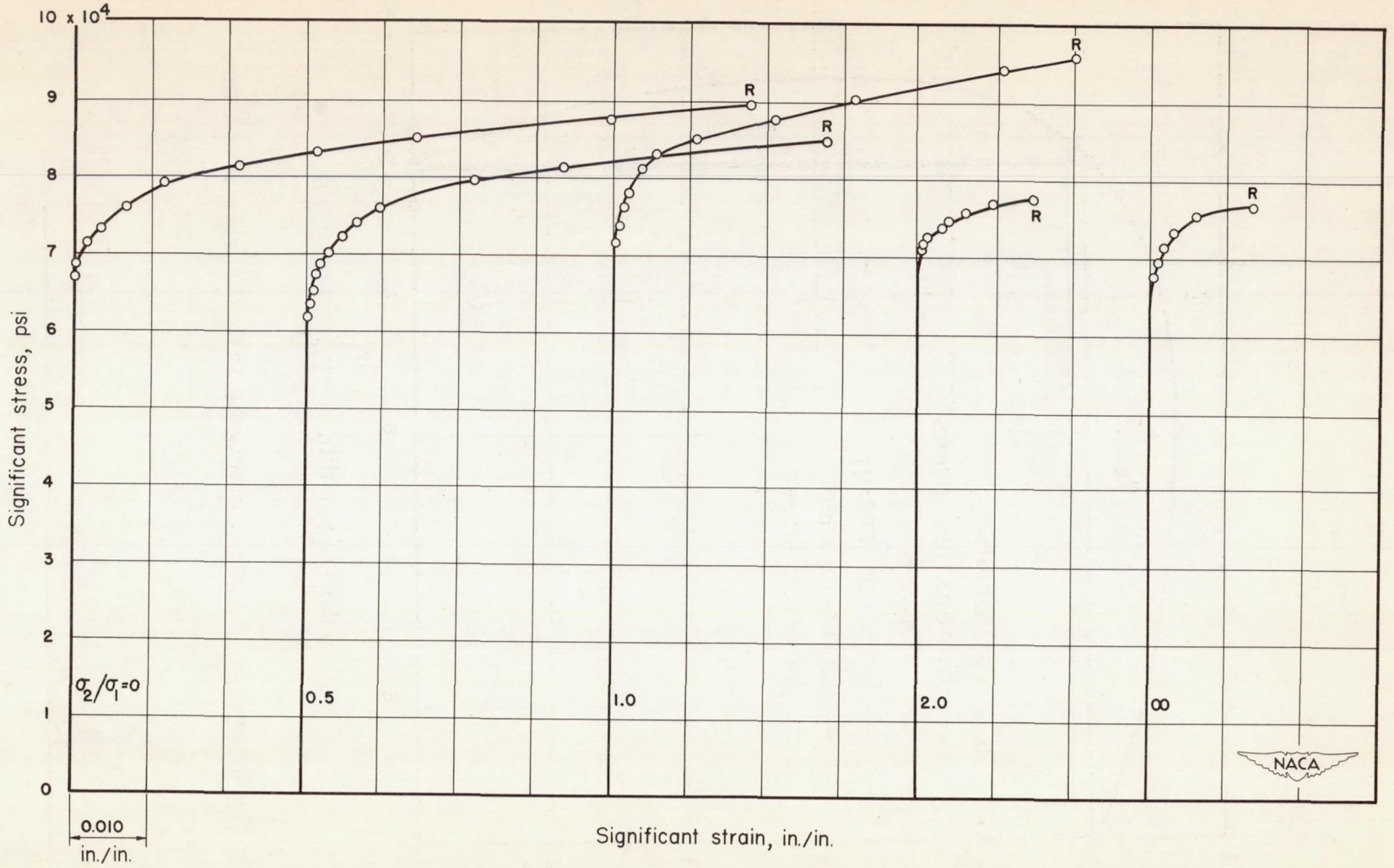

Figure 9.- Significant stress-strain relations for various constant principal stress ratios. R denotes rupture point.

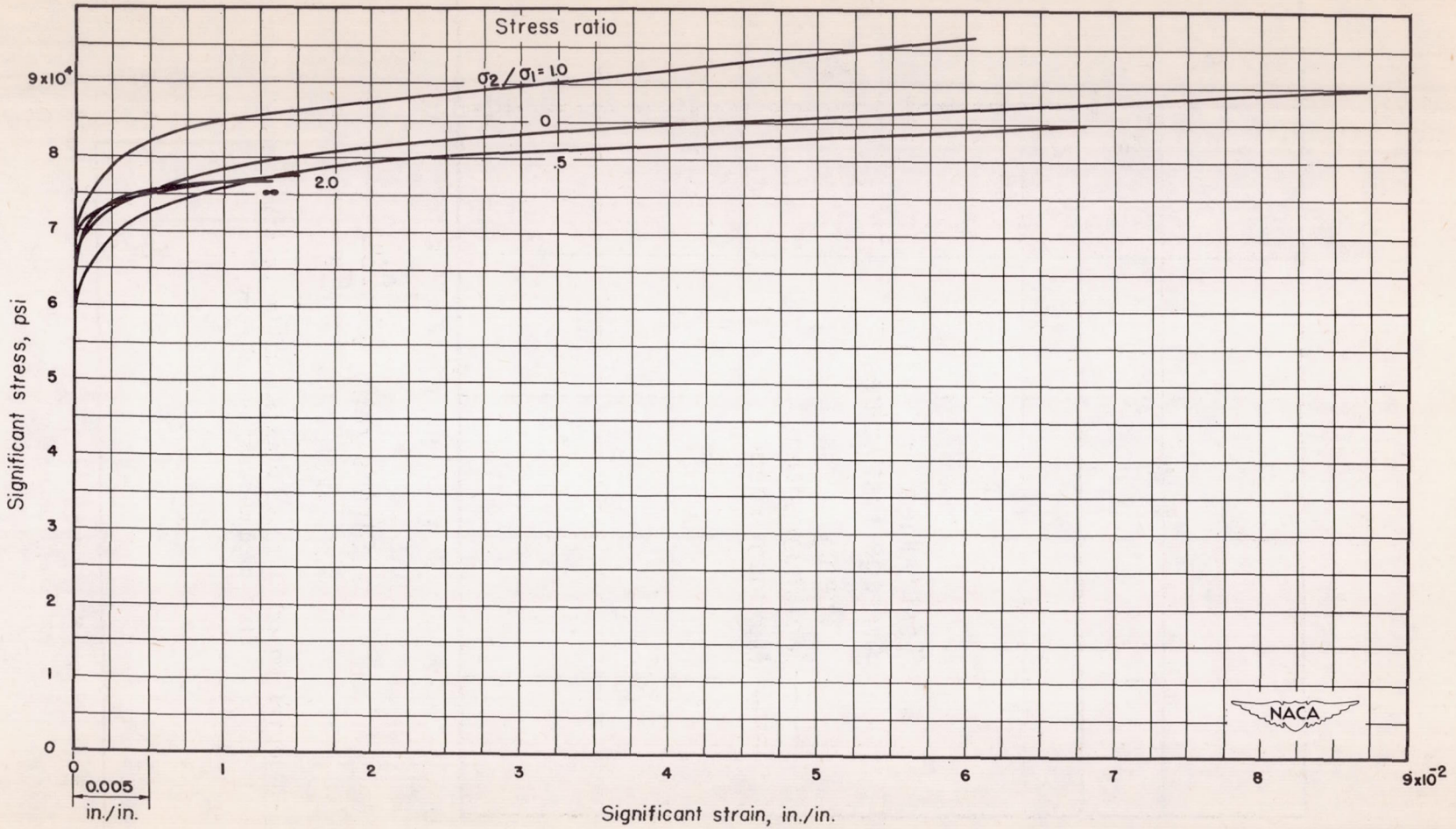

Figure 10.- Comparison of significant stress-strain relations with uniaxial true stress-strain values for constant stress ratios.

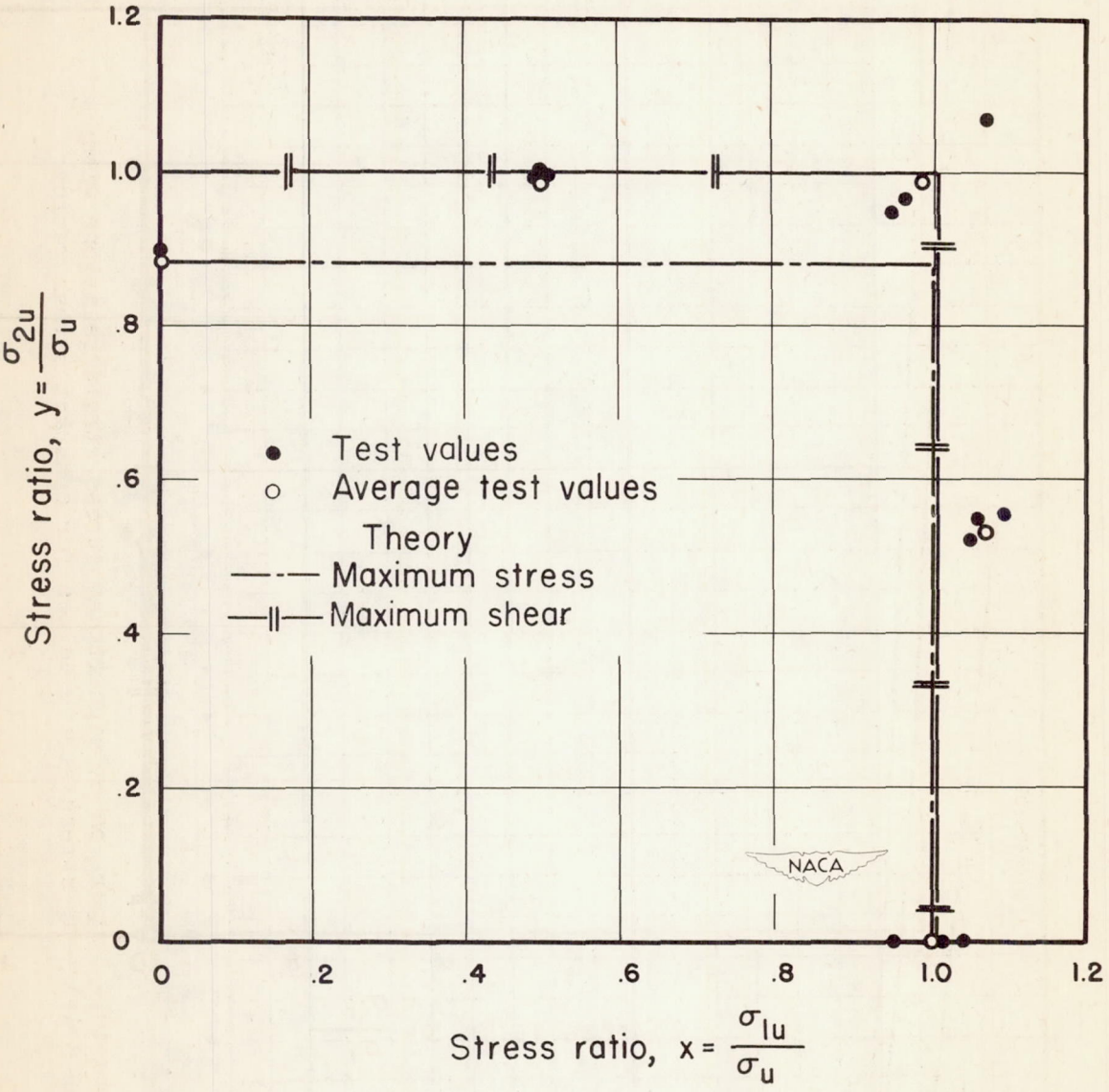

Figure 11.- Comparison of nominal biaxial ultimate stresses with values from maximum-stress theory.

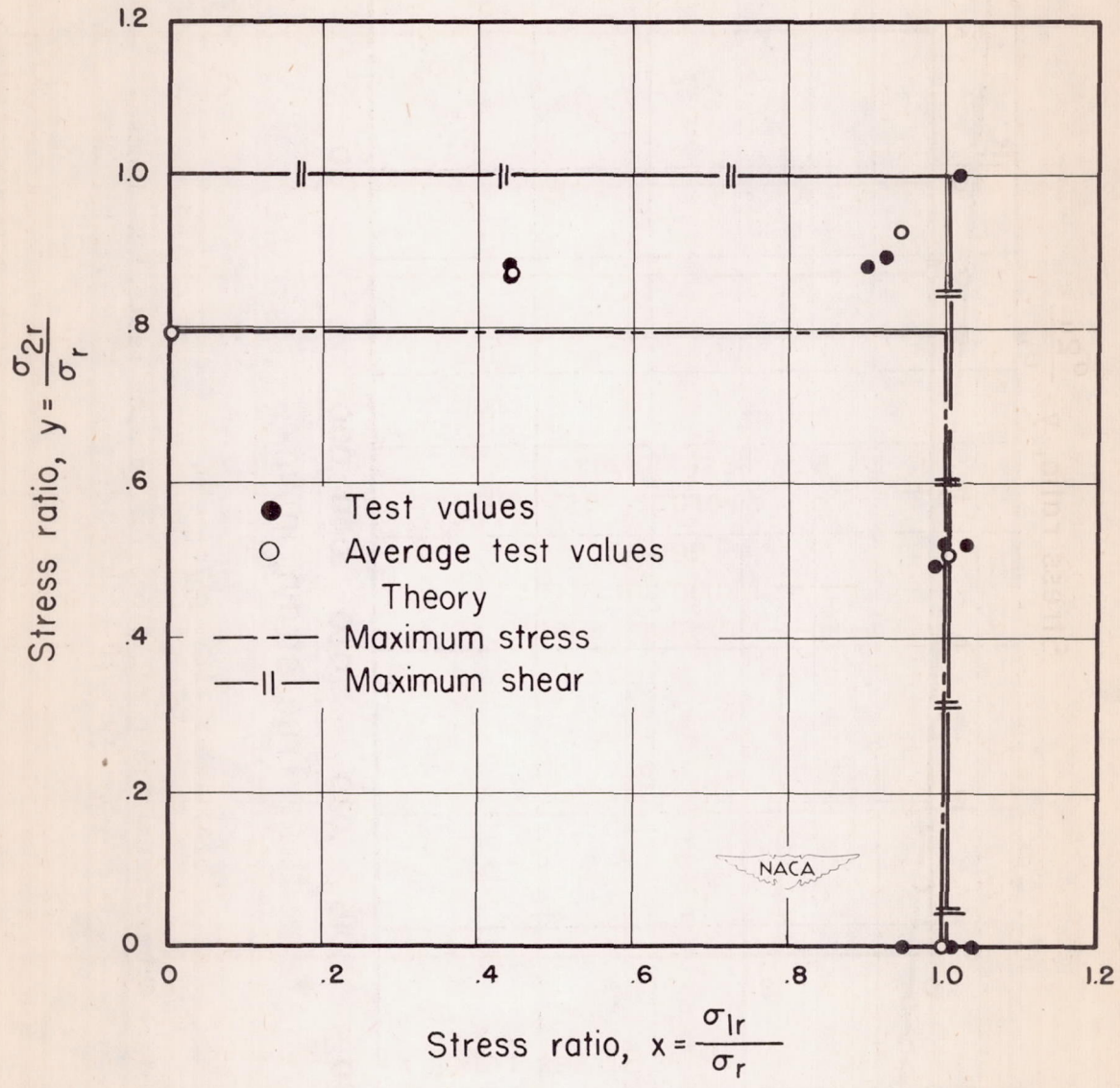

Figure 12.- Comparison of true biaxial fracture stresses with values from maximum-stress theory.

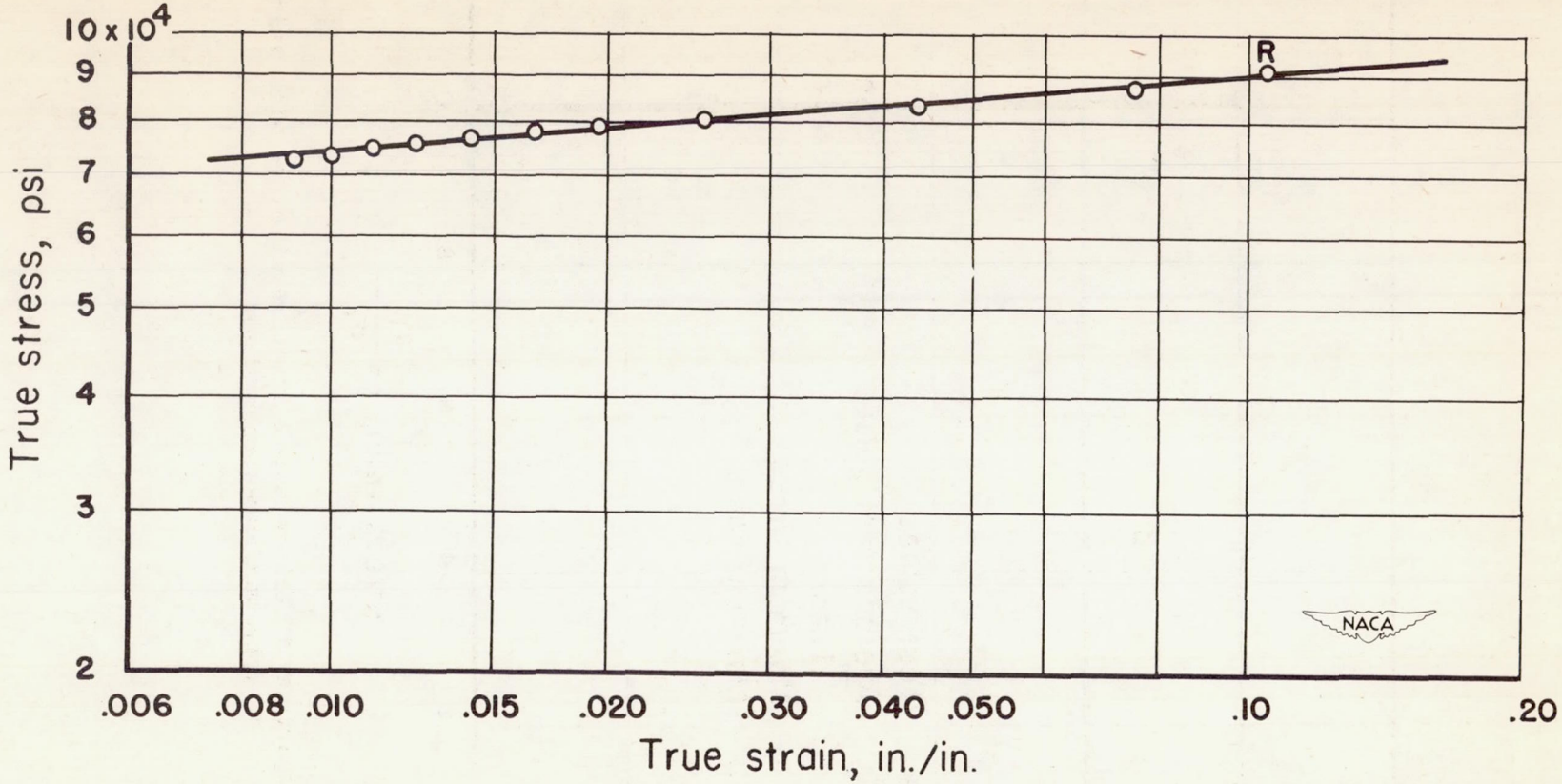

(a) Tubes with $\sigma_2/\sigma_1 = 0$.

Figure 13.- True stress-strain relations for tension tests. R denotes rupture point.

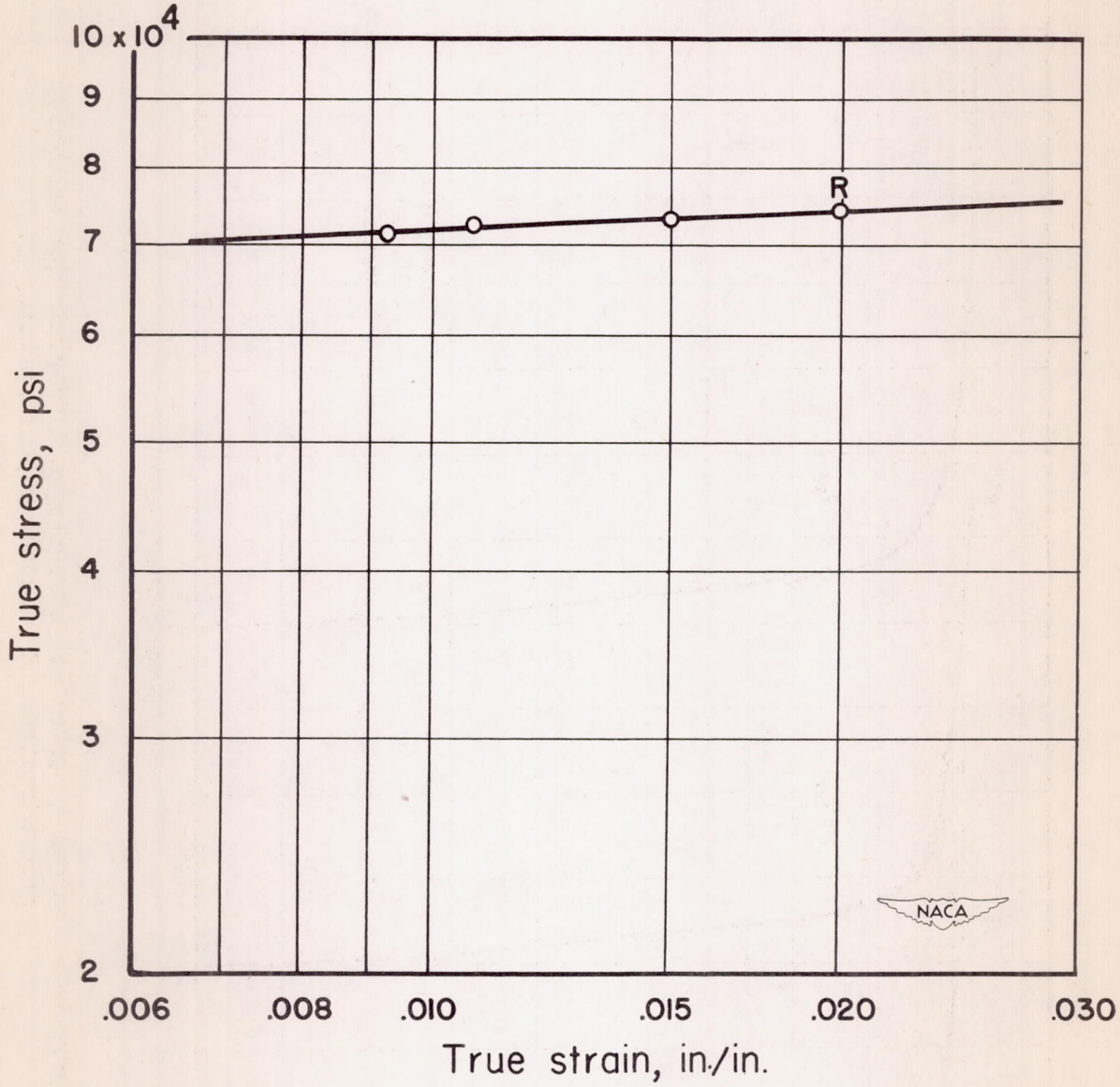

(b) Tubes with $\sigma_2/\sigma_1 = \infty$.

Figure 13.- Concluded.

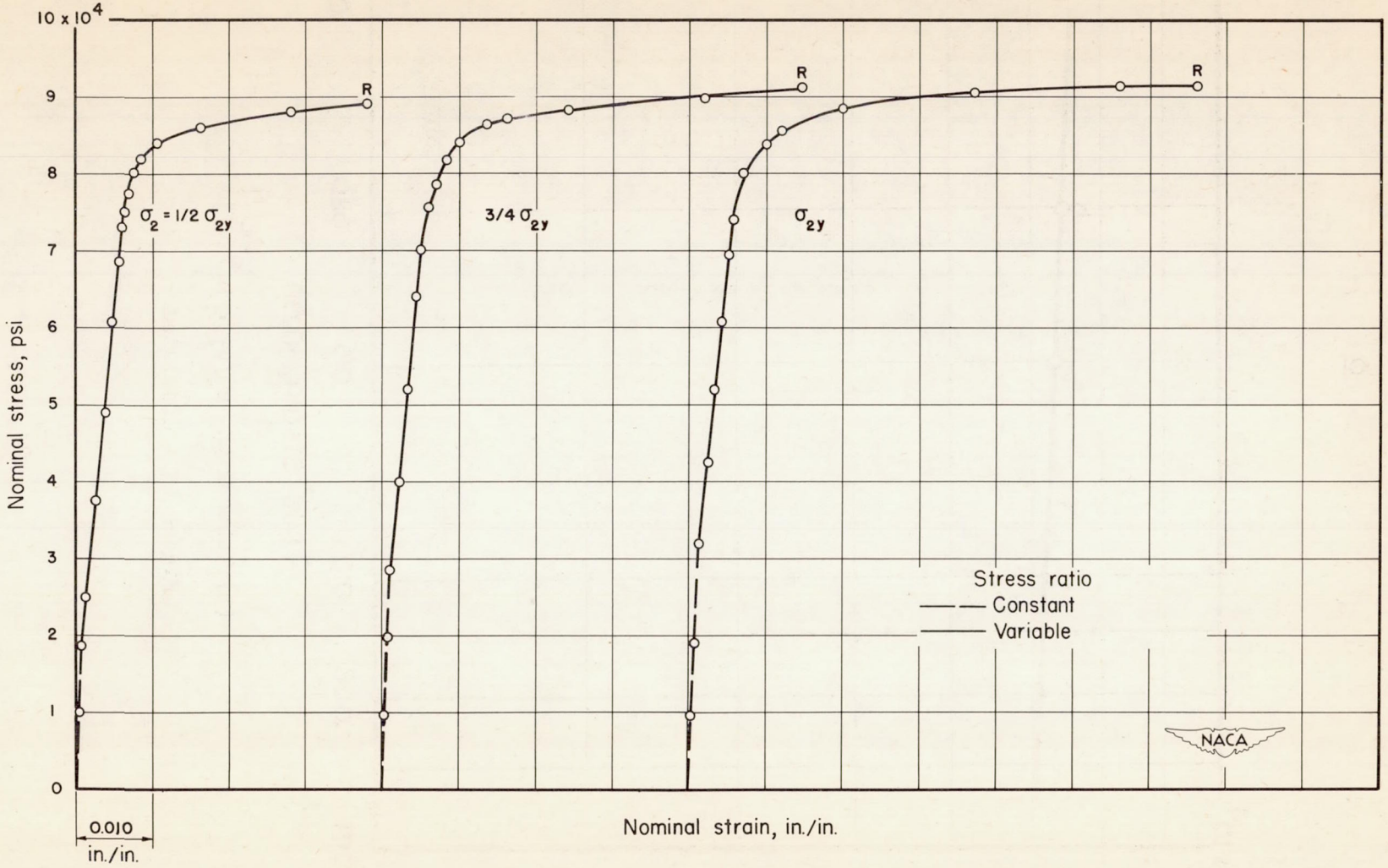

Figure 14.- Nominal longitudinal stress-strain diagrams for variable stress ratios. R denotes rupture point.

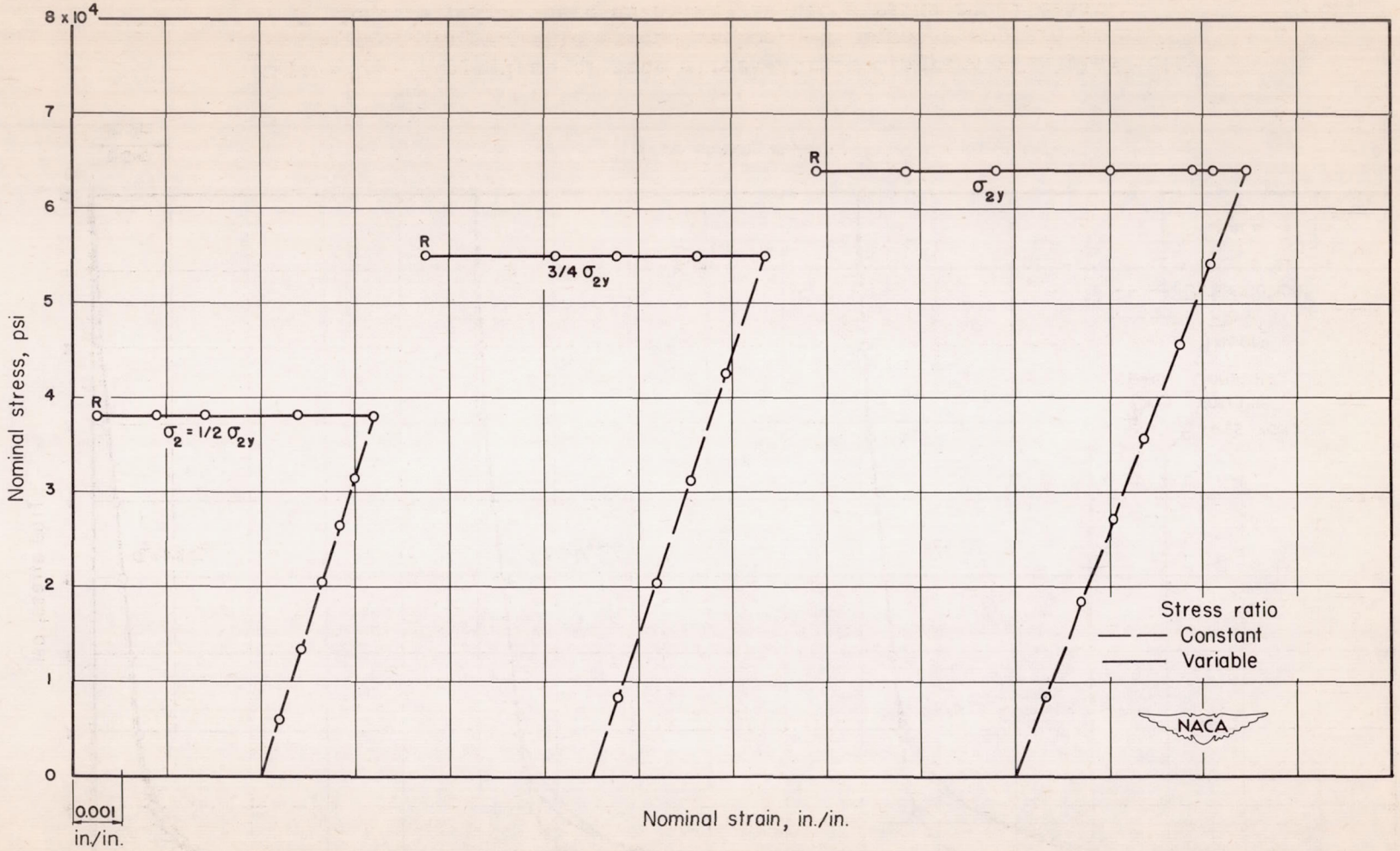

Figure 15.- Nominal lateral stress-strain relations for variable stress ratios. R denotes rupture point.

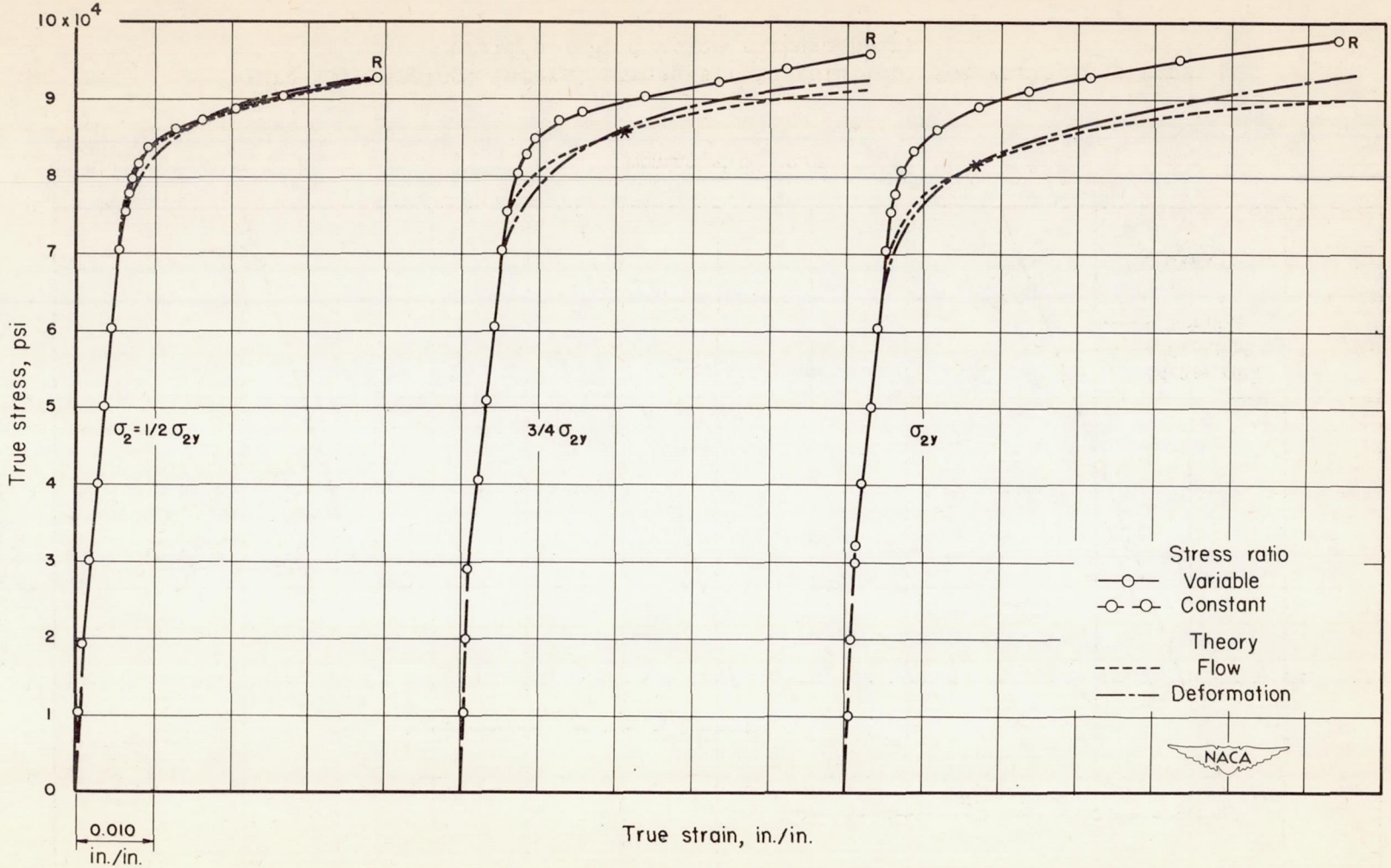

Figure 16.- Comparison of true stress-strain diagrams with plasticity theories for variable stress ratios. R denotes rupture point; * denotes point where uniaxial plastic strains equal elastic strains.

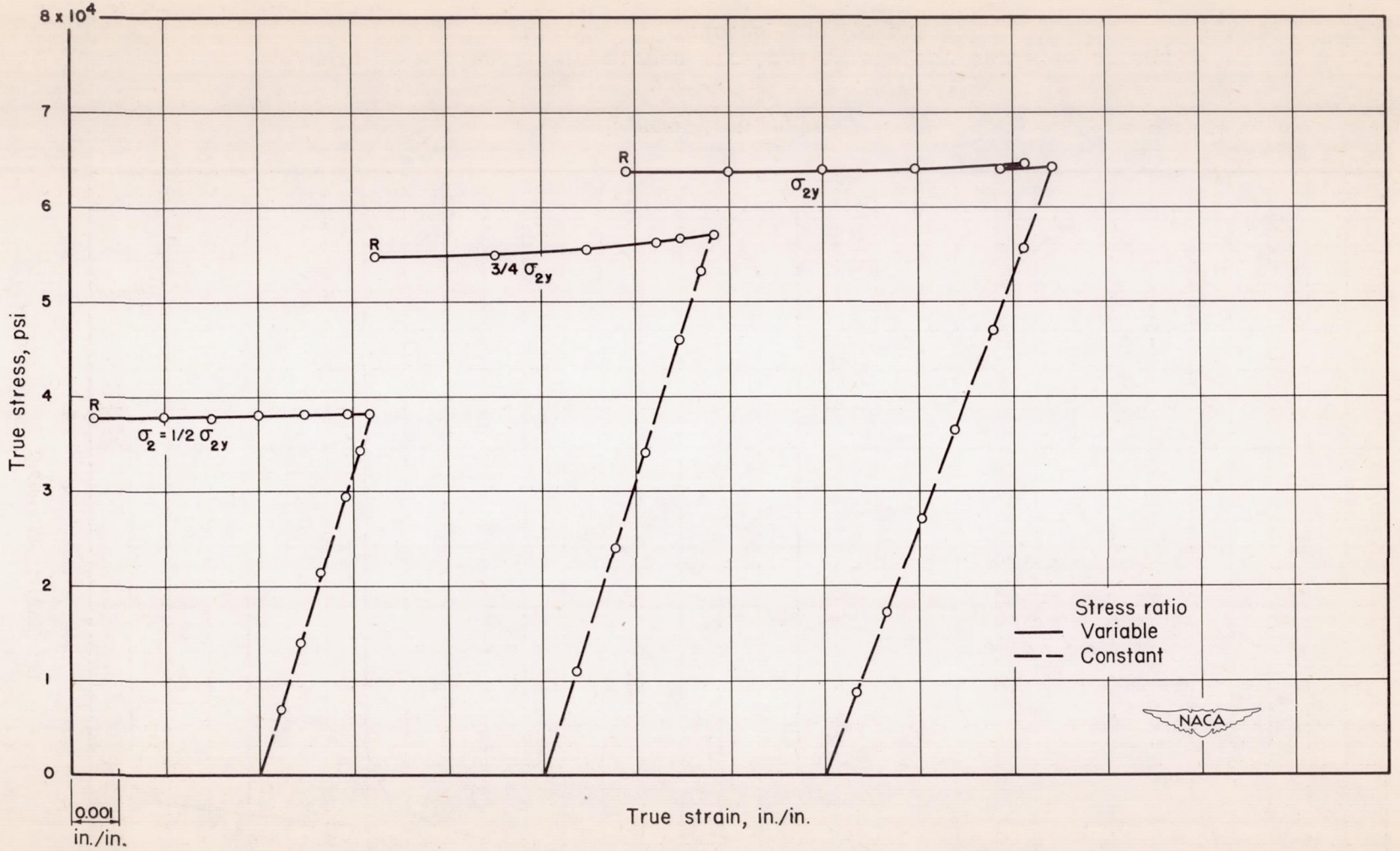

Figure 17.- True lateral stress-strain diagram for variable stress ratios.
R denotes rupture point.

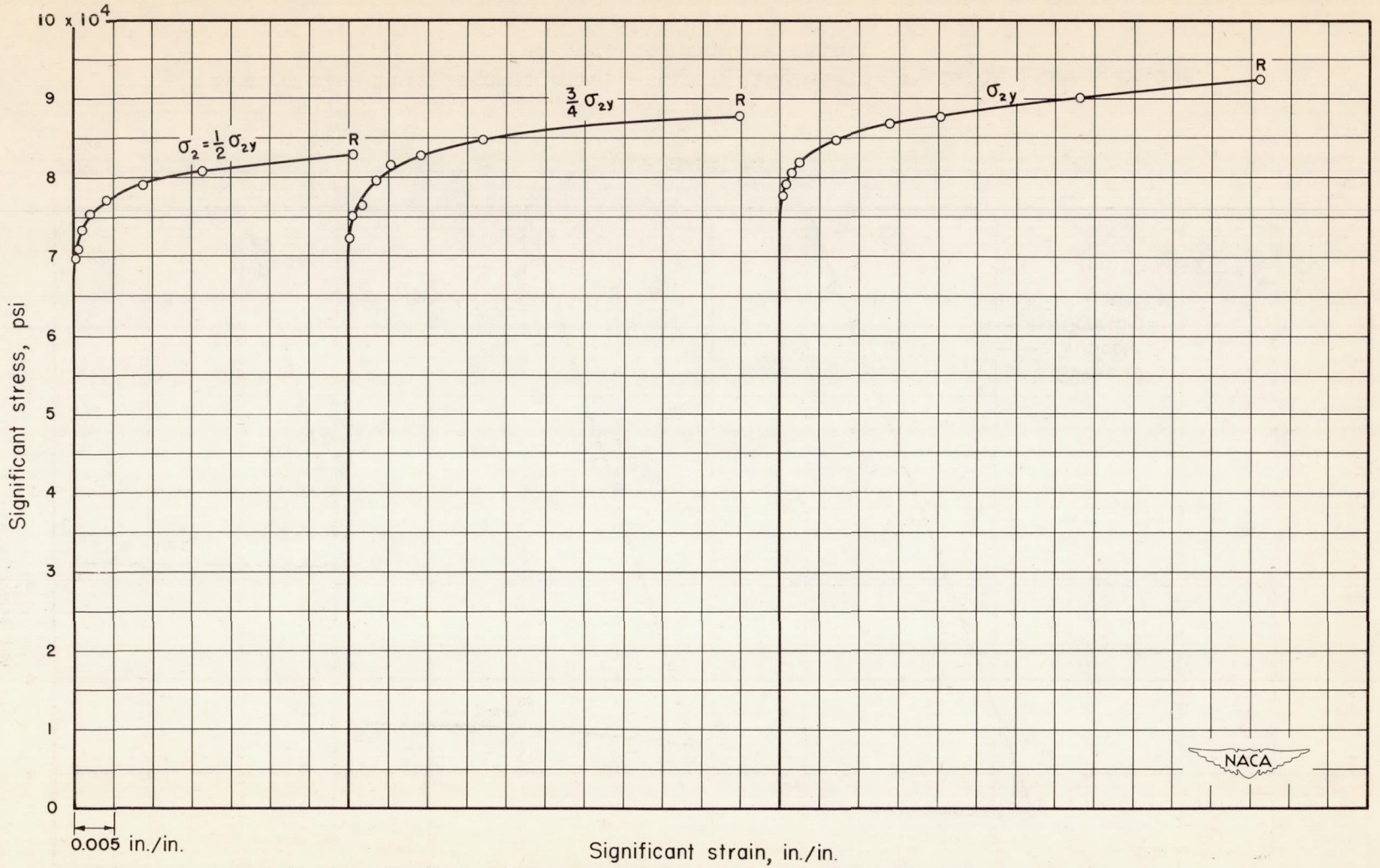

Figure 18.- Significant stress-strain diagrams for variable stress ratios. R denotes rupture point.

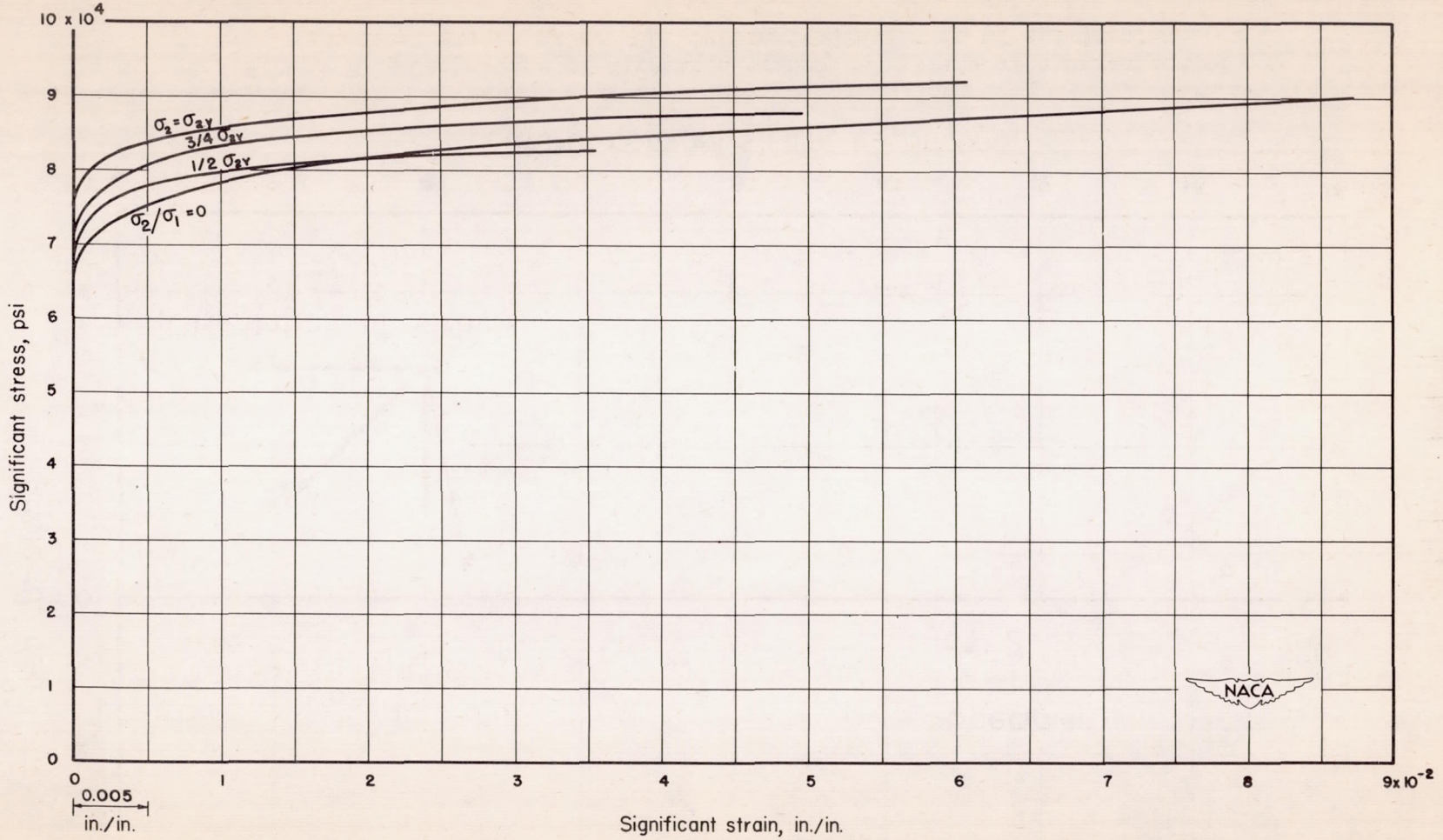

Figure 19.- Comparison of significant stress-strain relations with uniaxial true stress-strain values for variable stress ratios.

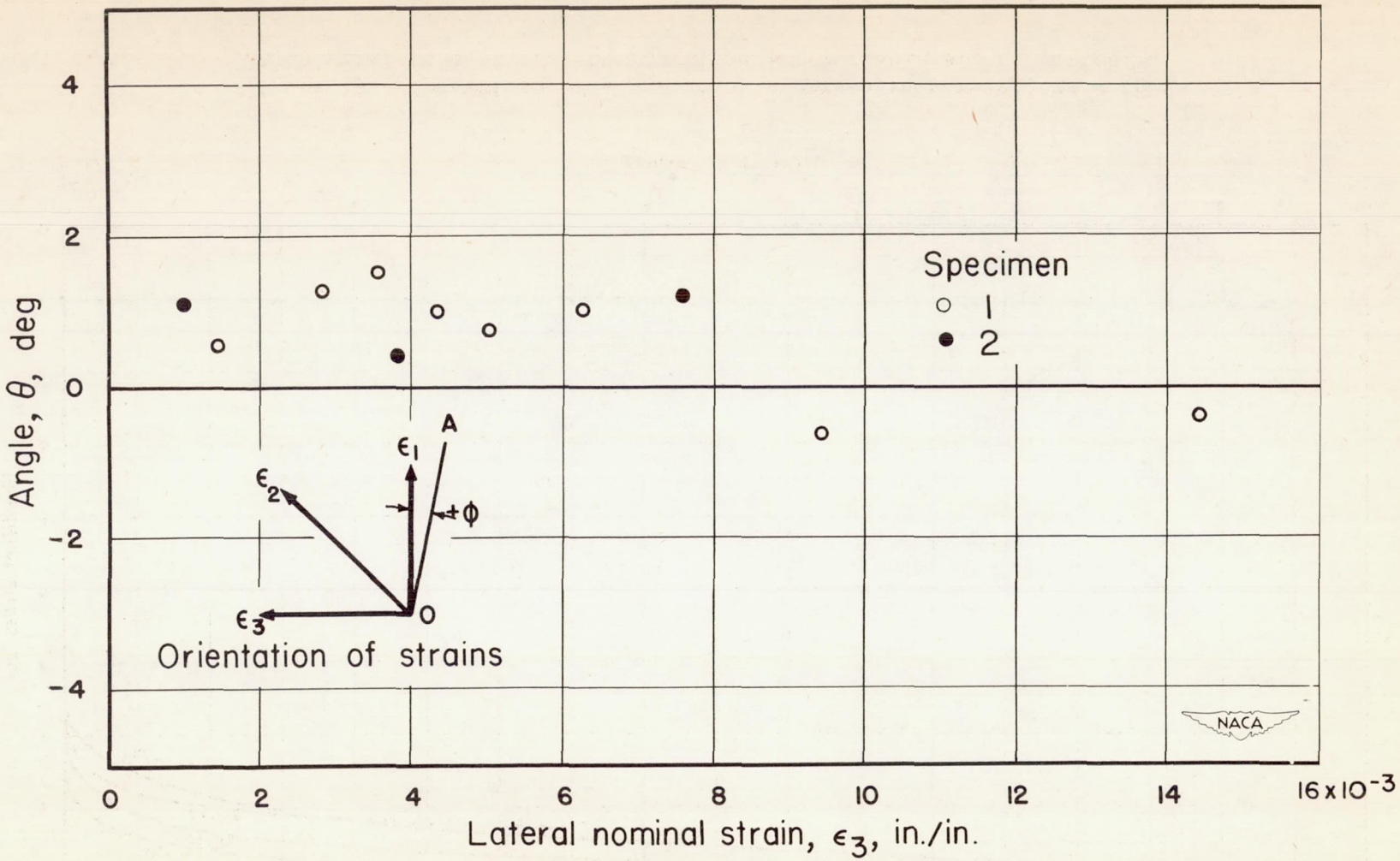

Figure 20.- Comparison of direction of nominal strain with direction of nominal stress axis. OA is longitudinal axis of specimen.

NACA-Langley - 8-15-51 - 1000